

Geometric phases in quantum information

Erik Sjöqvist*

October 8, 2015

Abstract

The rise of quantum information science has opened up a new venue for applications of the geometric phase (GP), as well as triggered new insights into its physical, mathematical, and conceptual nature. Here, we review this development by focusing on three main themes: the use of GPs to perform robust quantum computation, the development of GP concepts for mixed quantum states, and the discovery of a new type of topological phases for entangled quantum systems. We delineate the theoretical development as well as describe recent experiments related to GPs in the context of quantum information.

arXiv:1503.04847v2 [quant-ph] 7 Oct 2015

*Department of Quantum Chemistry, Uppsala University, Box 518, SE-751 20 Uppsala, SWEDEN

INTRODUCTION

A cat held upside down can fall on its feet although its angular momentum vanishes¹. An amoeba can swim in a completely reversibel environment². How do they manage?

The mechanism used by these cats and amoebae is the same as that used by a quantum state that returns to itself, but picks up a phase factor of geometric origin. The mechanism is called *holonomy* or *geometric phase* (GP) and describes the twisting of a physical quantity, such as the orientation of the cat or the phase of the quantum state, due to the curved geometry of the physical space where the change takes place³. This space is the space of shapes in the case of cats, while it is the quantum state space or projective Hilbert space in the case quantum states.

If the evolution of a quantum system is induced by slowly changing some external parameters around a loop, the state approximately performs a loop giving rise to an adiabatic GP. This kind of GP was first discovered in the field of quantum chemistry by Longuet-Higgins and coworkers⁴⁻⁶ and Stone⁷. It is the underlying mechanism behind the molecular Aharonov-Bohm effect^{8,9}, which takes the form of a topological phase shift when a molecule reshapes slowly around a conical intersection point.

Later, Berry¹⁰ demonstrated that the GP is a general consequence of the geometrical structure of the space of parameters that drive cyclic adiabatic evolution of energetically non-degenerate quantum states; a scenario that can be realized in numerous systems, such as photons¹¹, NMR¹², neutrons¹³, Jahn-Teller molecules¹⁴, condensed matter systems¹⁵, and cold atoms¹⁶. Simon¹⁷ demonstrated that Berry's GP can be understood as the holonomy in a Hermitian line bundle. This result has established the geometrical nature of the phase.

GPs have been generalized beyond Berry's framework. Wilczek and Zee¹⁸, still within the context of adiabatic evolution, pointed out that energetically degenerate states may aquire matrix-valued GPs when slowly changing parameters trace out a loop in parameter space. The matrix nature of these phases make them potentially non-commuting; a fact that has motivated the term non-Abelian GP or quantum holonomy for this kind of phase effects. Aharonov and Anandan¹⁹ removed the restriction of adiabatic evolution and introduced the concept of non-adiabatic GP in arbitrary cyclic quantum evolution. Subsequently,

Anandan²⁰ proposed non-adiabatic non-Abelian GPs of general quantum systems. Based on Panchartnam's work²¹ on polarization of classical light fields, Samuel and Bhandari²² defined GPs for open paths in the underlying state space.

The rise of quantum information science has opened up a new venue for application of the GP, namely, to use it as a tool for robust quantum information processing^{23,24}. This development has been triggered by the work of Zanardi and coworkers²⁵⁻²⁷ on *holonomic quantum computation*, i.e., the idea to use non-Abelian Wilczek-Zee GPs to implement quantum gates; the logical transformations that build up a circuit-based quantum computation. Such implementations are believed to be useful to reach the error threshold, below which quantum computation with faulty gates can be performed. The basic reasoning behind the conjectured robustness is that GP is a global feature of quantum evolution being resilient to errors, such as parameter noise and environment-induced decoherence, which are picked up locally along the path in state space.

Conversely, tools and concepts developed in quantum information theory have been used to broaden the concept of GP itself. Based on early work by Uhlmann²⁸ on holonomy along paths of density operators, new concepts of GPs for statistical mixtures of wave functions have been developed²⁹⁻³². In relation to these *mixed state geometric phases*, GPs of quantum systems that interact with a quantum-mechanical environment have been examined in the contexts of quantum jumps^{33,34}, quantum maps³⁵⁻³⁷, stochastic unravellings³⁸⁻⁴¹, and the adiabatic approximation⁴²⁻⁴⁴. Studies of GPs of two or more quantum degrees of freedom have led to the discovery of *entanglement-induced topological phases*⁴⁵⁻⁴⁷. This new type of phases have been shown to be useful to characterize quantum entanglement.

The objective of this review is to describe the recent merging of ideas in quantum information science and the field of GP. The basic theory of Abelian and non-Abelian GPs are outlined in the next section. Thereafter follows the core of this review, namely, a description and overview of various applications of GPs in quantum information. This part is focused on three main themes: quantum computation, mixed quantum states, and quantum entanglement. The paper ends with a concluding section, which in particular contains some pertinent issues to examine in the future in this research area.

DIFFERENT FLAVORS OF GEOMETRIC PHASE

The general structure of the quantum geometric phase (GP) is the removal of accumulated local phase changes from the global phase acquired in some evolution of a quantum system⁴⁸:

$$\text{GP} = \text{Global phase} - \sum \text{Local phase changes.} \quad (1)$$

The resulting GP factor can be an Abelian phase factor, denoted as $e^{i\Phi[\mathcal{C}]}$, or a non-Abelian unitary matrix, denoted as $U[\mathcal{C}]$, depending on the context. The path \mathcal{C} may reside in different kinds of spaces, such as projective Hilbert space in the case of pure states, the space of subspaces in the case of quantum gates, and the space of density operators in the case of mixtures of pure states. In this section, we review the basic theory of these Abelian and non-Abelian GPs by illustrating them in the physical context of pure state evolution.

Abelian GPs

A well-known feature of quantum evolution driven by a time-independent Hamiltonian H is that a stationary pure quantum state, as represented by a vector $|n\rangle$ in Hilbert space of the system, picks up a phase factor determined by the average energy $\langle n|H|n\rangle = E$ and the elapsed time t , i.e.,

$$|\psi(0)\rangle = |n\rangle \rightarrow |\psi(t)\rangle = e^{-iEt/\hbar}|n\rangle. \quad (2)$$

This simple fact is not true when the state itself evolves in time as the phase then picks up information of the geometry of the path in state space in addition to the system's energy. The origin of this extra phase contribution, being the pure state GP, is the curvature of state space.

To understand the appearance of a GP shift accompanying state changes, consider a superposition of two stationary states $|n\rangle$ and $|m\rangle$ of the form

$$|\psi(0)\rangle = a|n\rangle + b|m\rangle. \quad (3)$$

Let E_n and E_m be the corresponding energies assumed to be non-degenerate and ordered as $E_m > E_n$. The coefficients a and b are non-zero complex numbers whose values determine

the initial state of the system, such that $|a|^2$ and $|b|^2$ are the probabilities to find the energies E_n and E_m , respectively. Linearity of the Schrödinger equation implies that $|\psi(0)\rangle$ evolves into

$$|\psi(t)\rangle = ae^{-iE_n t/\hbar}|n\rangle + be^{-iE_m t/\hbar}|m\rangle. \quad (4)$$

This describes a non-trivial cyclic evolution of the quantum state as can be seen by evaluating $|\psi(t)\rangle$ at time $\tau = 2\pi\hbar/(E_m - E_n)$:

$$\begin{aligned} |\psi(\tau)\rangle &= e^{-iE_n \tau/\hbar} (a|n\rangle + be^{-i(E_m - E_n)\tau/\hbar}|m\rangle) \Big|_{t=\tau} \\ &= e^{-i2\pi E_n/(E_m - E_n)} |\psi(0)\rangle \equiv e^{if} |\psi(0)\rangle. \end{aligned} \quad (5)$$

τ is thus the period of the cyclic evolution that corresponds to the loop $\mathcal{C} : [0, \tau] \ni t \rightarrow |\psi(t)\rangle\langle\psi(t)|$ in state space.

The resulting overall phase $f = -2\pi E_n/(E_m - E_n)$ can be divided into a sum of two parts. The first part is the phase induced by the average energy $\langle\psi(t)|H|\psi(t)\rangle = |a|^2 E_n + |b|^2 E_m$ and reads

$$\delta = -\frac{2\pi}{E_m - E_n} (|a|^2 E_n + |b|^2 E_m) \quad (6)$$

in analogy with the above phase shift Et/\hbar for a stationary state. δ is clearly energy-dependent and therefore a dynamical phase associated with the evolution. The remainder $\gamma = f - \delta$ reads

$$\gamma = -\frac{2\pi E_n}{E_m - E_n} + \frac{2\pi}{E_m - E_n} (|a|^2 E_n + |b|^2 E_m) = 2\pi|b|^2, \quad (7)$$

where we have used normalization $|a|^2 + |b|^2 = 1$. Remarkably, γ is independent of the energies of the system; in fact, γ is the GP $\Phi[\mathcal{C}]$ associated with the loop \mathcal{C} .

If we remove the second phase factor $e^{-iE_m t/\hbar}$ instead of the phase factor $e^{-iE_n t/\hbar}$, then the overall phase $\tilde{f} = -2\pi E_m/(E_m - E_n)$ and the GP $\tilde{\gamma} = -2\pi|a|^2 \neq \gamma$. By using the normalization of $|\psi(0)\rangle$, we find $\gamma - \tilde{\gamma} = 2\pi$, which implies $e^{i\tilde{\gamma}} = e^{i\gamma}$. In other words, the GP factor is the same for the two arbitrary phase choices. Indeed, it is not difficult to prove that it is invariant under any phase choice of the evolving state, which makes the GP of a pure state an invariant under the Abelian group $U(1)$, i.e., the group of phase transformations.

The independence of energy and local phase choice suggest that the Abelian GP can be defined without reference to the underlying dynamical mechanism that drives the evolution. This can be seen by using the concept of relative phase²¹ between state vectors. Let $|\psi(t_1)\rangle$ and $|\psi(t_2)\rangle$ be two non-orthogonal vectors along a continuous curve $C : t \in [0, \tau] \rightarrow |\psi(t)\rangle$ in Hilbert space. The phase of $|\psi(t_2)\rangle$ relative $|\psi(t_1)\rangle$ is simply the phase of the scalar product $\langle\psi(t_1)|\psi(t_2)\rangle$. The relative phase concept can be used to define

$$\text{Global phase} = \arg\langle\psi(0)|\psi(\tau)\rangle, \quad (8)$$

being well-defined if $\langle\psi(0)|\psi(\tau)\rangle \neq 0$ (non-orthogonal end-points), and

$$\sum \text{Local phase changes} = \lim_{\delta t \rightarrow 0} \int_0^\tau \arg\langle\psi(t)|\psi(t + \delta t)\rangle = -i \int_0^\tau \langle\psi(t)|\dot{\psi}(t)\rangle dt, \quad (9)$$

where we have used Taylor expansion $\langle\psi(t)|\psi(t + \delta t)\rangle \approx 1 + \langle\psi(t)|\dot{\psi}(t)\rangle\delta t \approx e^{\langle\psi(t)|\dot{\psi}(t)\rangle\delta t}$ and the fact that $\langle\psi(t)|\dot{\psi}(t)\rangle$ is purely imaginary due to normalization: $1 = \langle\psi(t)|\psi(t)\rangle \Rightarrow 0 = \langle\dot{\psi}(t)|\psi(t)\rangle + \langle\psi(t)|\dot{\psi}(t)\rangle = 2\text{Re}\langle\psi(t)|\dot{\psi}(t)\rangle$. By combining Eqs. (8) and (9) with Eq. (1), we obtain⁴⁸

$$\Phi[\mathcal{C}] = \arg\langle\psi(0)|\psi(\tau)\rangle + i \int_0^\tau \langle\psi(t)|\dot{\psi}(t)\rangle dt. \quad (10)$$

This GP is invariant under local phase changes $|\psi(t)\rangle \rightarrow e^{i\alpha(t)}|\psi(t)\rangle$ and invariant under reparametrizations $t \rightarrow \tau(t)$ such that $\dot{\tau} > 0, \forall t \in [0, \tau]$. Thus, GP is a property of the path \mathcal{C} in state space, defined by the projection $|\psi(t)\rangle \rightarrow |\psi(t)\rangle\langle\psi(t)|$ of the path C in Hilbert space. Note that this definition of GP makes no reference to cyclic evolution and therefore applies to any evolution of a pure quantum state connecting two non-orthogonal end-points $|\psi(0)\rangle$ and $|\psi(\tau)\rangle$.

There are three ‘canonical’ choices of local phase:

- (i) If $|\psi(t)\rangle$ is a solution of the Schrödinger equation, i.e., satisfies $i\hbar|\dot{\psi}(t)\rangle = H(t)|\psi(t)\rangle$, then we obtain from Eq. (10) the expression¹⁹

$$\Phi[\mathcal{C}] = \arg\langle\psi(0)|\psi(\tau)\rangle - \frac{1}{\hbar} \int_0^\tau \langle\psi(t)|H(t)|\psi(t)\rangle dt, \quad (11)$$

where $H(t)$ is the Hamiltonian of the system. Thus, the GP can be understood as the removal of the accumulated phase induced by the average energy $\langle\psi(t)|H(t)|\psi(t)\rangle$, i.e.,

the dynamical phase shift of the system, from the acquired global phase, just as in the example of the two superposed stationary states discussed above.

(ii) If

$$\langle \psi(t) | \psi(t + \delta t) \rangle > 0 \Rightarrow \langle \psi(t) | \dot{\psi}(t) \rangle = 0, \quad t \in [0, \tau) \quad (12)$$

no phase changes are acquired along the path, and we obtain

$$\Phi[\mathcal{C}] = \arg \langle \psi(0) | \psi(\tau) \rangle. \quad (13)$$

When Eq. (12) is satisfied, $|\psi(t)\rangle$ is said to be parallel transported. In this case, the GP coincides with the global phase associated with the evolution. Parallel transport is particularly useful in experiments as it makes the GP directly accessible by observing the global phase^{49–51}.

(iii) The phase choice $|\lambda(t)\rangle = e^{-i \arg \langle \psi(0) | \psi(t) \rangle} |\psi(t)\rangle$ is a gauge invariant reference section^{52,53} as $|\lambda(t)\rangle$ is unchanged under local phase transformations of $|\psi(t)\rangle$. (To be precise, $|\lambda(t)\rangle \rightarrow e^{i\alpha(t)} |\lambda(t)\rangle$ when $|\psi\rangle \rightarrow e^{i\alpha(t)} |\psi(t)\rangle$.) We note that $\arg \langle \lambda(0) | \lambda(\tau) \rangle$ vanishes so that

$$\Phi[\mathcal{C}] = i \int_0^\tau \langle \lambda(t) | \dot{\lambda}(t) \rangle dt, \quad (14)$$

which is the familiar form of the geometric phase being the closed path integral of the effective ‘vector potential’ $i\langle \lambda | d\lambda \rangle$. This perspective was adopted in Berry’s original work on GP¹⁰.

Note that although the three canonical phase choices focus on different aspects of quantum evolution, they differ only by local phase choices and therefore all give the same numerical result for the GP.

Example: GP of a qubit

A qubit is a quantum system that can be described by two states $|0\rangle$ and $|1\rangle$. Physical examples of qubits are abundant: it could be the polarization of a photon, the spin of an

electron, neutron, or proton, two isolated states of an atom or ion, two charge state of a superconducting island, and so on. An arbitrary qubit state $|\psi\rangle$ can be written as

$$|\psi\rangle = \cos\frac{\theta}{2}|0\rangle + e^{i\phi}\sin\frac{\theta}{2}|1\rangle. \quad (15)$$

The two parameters θ and ϕ may be interpreted as polar angles of a unit sphere, called the Bloch sphere, with $|0\rangle$ and $|1\rangle$ projecting onto the north ($\theta = 0$) and south poles ($\theta = \frac{\pi}{2}$), respectively, see Figure 1.

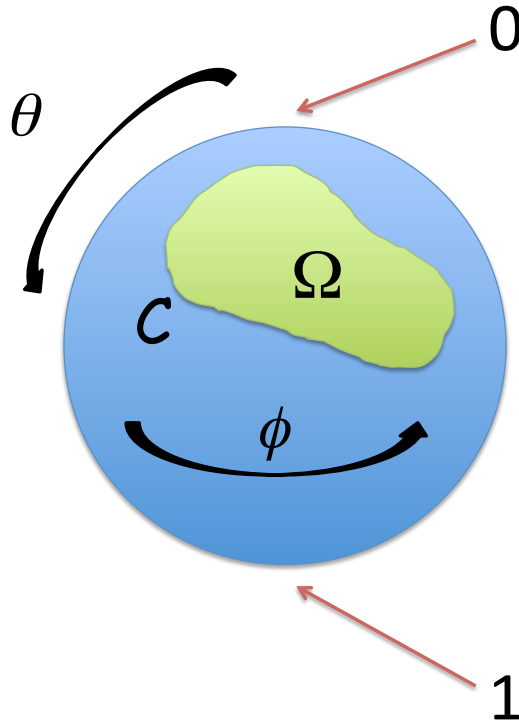


Figure 1: Bloch sphere representing pure qubit states with the projection of the basis states $|0\rangle$ and $|1\rangle$ at the poles. The angles θ and ϕ determine the relative weight and phase shift, respectively, between $|0\rangle$ and $|1\rangle$. A loop \mathcal{C} enclosing the solid angle Ω on the Bloch sphere is associated with the GP $-\frac{1}{2}\Omega$.

Now, by assuming that the qubit traces out a loop $\mathcal{C} : t \in [0, \tau] \rightarrow (\theta_t, \phi_t)$ on the Bloch

sphere, i.e., $\theta_\tau = \theta_0$ and $\phi_\tau = \phi_0$, we obtain

$$\Phi[\mathcal{C}] = -\frac{1}{2} \oint_{\mathcal{C}} (1 - \cos \theta) d\phi = -\frac{1}{2} \Omega, \quad (16)$$

Ω being the solid angle enclosed on the Bloch sphere by \mathcal{C} . By using Stokes theorem, we obtain

$$\Phi[\mathcal{C}] = -\frac{1}{2} \oint_{\mathcal{S}} \sin \theta d\theta d\phi \quad (17)$$

where \mathcal{S} is the surface on the Bloch sphere enclosed by \mathcal{C} . This is equivalent to the flux through \mathcal{S} of a magnetic monopole of strength $-\frac{1}{2}$ sitting at the origin.

Non-Abelian GPs

Following Berry's work¹⁰ on Abelian GP factors accompanying adiabatic changes, Wilczek and Zee¹⁸ pointed out that non-Abelian gauge structures appear when more than one state is considered. This turns out to be relevant for instance in adiabatic evolution where several energy eigenstates are degenerate over some region of parameter space.

The key ingredient of the non-Abelian generalization is the evolution of a subspace of the full state space. Let $t \in [0, \tau] \rightarrow \mathcal{S}_t$ trace out a loop \mathcal{C} (i.e., $\mathcal{S}_\tau = \mathcal{S}_0$) of K -dimensional subspaces of an N -dimensional Hilbert space. Let $\{|\psi_k(t)\rangle\}_{k=1}^K$ span \mathcal{S}_t . Since \mathcal{C} is a loop, the overlap matrix $\mathbf{U}_{kl}(0, \tau) = \langle \psi_k(0) | \psi_l(\tau) \rangle$ is unitary and corresponds to the overall 'phase' of the evolution. By applying the same reasoning for two infinitesimally close instances t and $t + \delta t$, we obtain the local 'phase shift' $e^{i\mathbf{A}(t)\delta t}$ to first order in δt . Here, $\mathbf{A}_{kl}(t) = i\langle \psi_k(t) | \dot{\psi}_l(t) \rangle$. The accumulated local phase shift along the loop is $\mathcal{T} e^{i \int_0^\tau \mathbf{A}(t) dt}$, where \mathcal{T} stands for time ordering. Thus, we obtain the non-Abelian GP:

$$\mathbf{U}[\mathcal{C}] = \mathbf{U} \mathcal{T} e^{i \int_0^\tau \mathbf{A}(t) dt}, \quad (18)$$

where $\mathbf{U} \equiv \mathbf{U}(0, \tau)$. Note that for the special case where $K = 1$, $\mathbf{U}[\mathcal{C}]$ reduces to the complex number

$$U[\mathcal{C}] = e^{i \arg \langle \psi(0) | \psi(\tau) \rangle} e^{-\int_0^\tau \langle \dot{\psi}(t) | \psi(t) \rangle dt} = e^{i(\arg \langle \psi(0) | \psi(\tau) \rangle + \int_0^\tau \langle \dot{\psi}(t) | \psi(t) \rangle dt)}, \quad (19)$$

which we recognize as the Abelian GP factor $e^{i\Phi[\mathcal{C}]}$ discussed above.

The subspace need not trace out a loop to acquire a non-Abelian GP. For such an open path \mathcal{C} , the overlap matrix $\mathbf{M}_{kl}(0, \tau) = \langle \psi_k(0) | \psi_l(\tau) \rangle$ is no longer unitary, but admits a unique polar decomposition $\mathbf{M} = |\mathbf{M}|\mathbf{U}$ provided $|\mathbf{M}| > 0$. We therefore have

$$\mathbf{M}\mathcal{T}e^{i\int_0^\tau \mathbf{A}(t)dt} = |\mathbf{M}|\mathbf{U}\mathcal{T}e^{i\int_0^\tau \mathbf{A}(t)dt} \equiv |\mathbf{M}|\mathbf{U}[\mathcal{C}], \quad (20)$$

which defines the non-Abelian GP⁵⁴

$$\mathbf{U}[\mathcal{C}] = |\mathbf{M}|^{-1}\mathbf{M}\mathcal{T}e^{i\int_0^\tau \mathbf{A}(t)dt} \quad (21)$$

valid for any evolution connecting two fully overlapping K -dimensional subspaces \mathcal{S}_0 and \mathcal{S}_τ of the N -dimensional Hilbert space. Note that the existence of the inverse $|\mathbf{M}|^{-1}$ is a consequence of the condition $|\mathbf{M}| > 0$ that is required for a unique polar decomposition of the overlap matrix.

The matrix-valued GPs may as well be viewed as operators:

$$U[\mathcal{C}] = \sum_{k,l=1}^K \mathbf{U}_{kl}[\mathcal{C}] |\psi_k(\tau)\rangle \langle \psi_l(0)|, \quad (22)$$

with initial subspace as domain and final subspace as image (these subspaces coincide if \mathcal{C} is a loop). The matrix and operator forms of the non-Abelian GPs are fully equivalent.

The non-Abelian GP transforms as $\mathbf{U}[\mathcal{C}] \rightarrow \mathbf{V}(0)\mathbf{U}[\mathcal{C}]\mathbf{V}^\dagger(0)$ under a unitary change of basis $|\psi_k(t)\rangle \rightarrow \sum_l |\psi_l(t)\rangle V_{lk}(t)$ along the moving subspace \mathcal{S}_t . This implies that the Wilson loop $\text{Tr}\mathbf{U}[\mathcal{C}]$ is unchanged under local basis changes. Thus, the non-Abelian GP transforms gauge covariantly and is therefore a property of the path \mathcal{C} in the space of subspaces⁵⁴.

Example: Geometric transformation of a qubit

A technical complication when calculating the non-Abelian GP is the need to evaluate a time-ordered product. This may be dealt with by performing a pair of loops resulting in non-commuting GPs, therefore demonstrating the desired non-Abelian feature, but along each of these loops no time-ordering is needed. Here, we illustrate this idea in the case of a two-dimensional subspace \mathcal{S} , encoding a single qubit, that evolves in a three-dimensional Hilbert space \mathcal{H} .

Let $\mathcal{H} = \text{Span}\{|0\rangle, |1\rangle, |a\rangle\}$. Consider paths of two-dimensional subspaces $\mathcal{C} \rightarrow \mathcal{S}_t = \text{Span}\{|\psi(t)\rangle, |\psi^\perp(t)\rangle\}$ such that \mathcal{S}_0 is the qubit subspace. Thus, $\mathcal{S}_0 = \text{Span}\{|0\rangle, |1\rangle\}$.

Let us first consider the choice

$$\begin{aligned} |\psi_1(t)\rangle &= |0\rangle, \\ |\psi_1^\perp(t)\rangle &= \cos \frac{\kappa_t}{2} |1\rangle + e^{i\eta_t} \sin \frac{\kappa_t}{2} |a\rangle. \end{aligned} \quad (23)$$

A loop \mathcal{C}_1 that starts and ends at \mathcal{S}_0 is implemented by choosing $\kappa_\tau = \kappa_0 = 0$ and $\eta_\tau = \eta_0$. The GP associated with \mathcal{C}_1 is

$$U[\mathcal{C}_1] = e^{-i|1\rangle\langle 1| \oint_{\mathcal{C}_1} (1 - \cos \kappa) d\eta}. \quad (24)$$

The phase shift can be interpreted as the solid angle enclosed on the Bloch sphere associated with the subspace $\text{Span}\{|1\rangle, |a\rangle\}$ and parametrized by the spherical polar angles κ, η .

Now, consider instead the choice

$$\begin{aligned} |\psi_2(t)\rangle &= -\sin \eta_t |0\rangle + \cos \eta_t |1\rangle, \\ |\psi_2^\perp(t)\rangle &= \cos \kappa_t \cos \eta_t |0\rangle + \cos \kappa_t \sin \eta_t |1\rangle - \sin \kappa_t |a\rangle, \end{aligned} \quad (25)$$

which span a subspace that starts and ends at \mathcal{S}_0 provided $\kappa_\tau = \kappa_0 = 0$ and $\eta_\tau = \eta_0$. The GP associated with this loop \mathcal{C}_2 is

$$U[\mathcal{C}_2] = e^{-i\sigma_y \oint_{\mathcal{C}_2} (1 - \cos \kappa) d\eta}, \quad (26)$$

where $\sigma_y = -i|0\rangle\langle 1| + i|1\rangle\langle 0|$. Just as $U[\mathcal{C}_1]$, the unitary qubit transformation $U[\mathcal{C}_2]$ has a geometric interpretation in terms of a solid angle but with a different meaning: it is the solid angle enclosed on a parameter sphere that defines all possible choices of two-dimensional subspaces with real-valued coefficients with respect to the given reference basis $\{|0\rangle, |1\rangle, |a\rangle\}$ of the full Hilbert space.

For non-trivial loops \mathcal{C}_1 and \mathcal{C}_2 the resulting $U[\mathcal{C}_1]$ and $U[\mathcal{C}_2]$ are non-commuting thereby demonstrating the desired non-Abelian feature of these GPs. The above qubit GPs were discovered theoretically by Unanyan *et al.*⁵⁵ in the context of atoms controlled by stimulated Raman adiabatic passage (STIRAP) techniques.

QUANTUM COMPUTATION

A classical computer works by manipulating a set of bits according to some algorithm to produce a desired result. Analogously, a quantum computer manipulates qubits by applying a certain combination of logical operations, quantum gates, forming a quantum circuit. GPs have been proposed to be useful in realizing quantum gates. One of the main reasons for considering GP-based quantum gates is that they are believed to be more robust than traditional dynamical gates, and therefore useful in order to reach the error threshold⁵⁶, below which quantum computation with faulty gates can be performed by means of error correction protocols^{57,58}.

A key ingredient of circuit-based quantum computation is the concept of universality, which is the ability to perform an arbitrary unitary transformation on a certain set of qubits. It has been shown that universality can be achieved by applying arbitrary single-qubit operations and at least one entangling two-qubit gate⁵⁹. An arbitrary single-qubit operation requires the ability to perform non-commuting gates. Geometric quantum computation (GQC) is the idea to use GPs to implement such a universal set of one- and two-qubit gates.

There is basically two different methods to achieve universality by using GPs. Either, one realizes geometric phase shift gates with respect to different bases^{60,61}, or one realizes non-commuting gates by using non-Abelian GPs for $K > 1$ dimensional subspaces^{25,62}. Each of these methods can be implemented by employing adiabatic or non-adiabatic evolution.

GQC based on Abelian GPs

Geometric phase shift gates take the form $|k\rangle \rightarrow e^{if_k} |k\rangle$ with f_k being the GP of the computational state $|k\rangle$. At first sight, such gates are not sufficient for universality since they all commute. To resolve this, one may instead implement GPs with respect to different bases^{60,61}. The resulting phase shift gates become non-commuting and therefore potentially universal.

To demonstrate this idea, consider a single-qubit $|k\rangle$, $k = 0, 1$. Assume the orthogonal states $|+\rangle = \cos \frac{\theta}{2} |0\rangle + e^{i\phi} \sin \frac{\theta}{2} |1\rangle$ and $|-\rangle = -e^{-i\phi} \sin \frac{\theta}{2} |0\rangle + \cos \frac{\theta}{2} |1\rangle$ acquire purely GP shifts $\mp \Omega/2$ after cyclic evolution (Ω being the solid angle enclosed by the Bloch vector). Thus,

$|\pm\rangle \rightarrow e^{\mp i\Omega/2}|\pm\rangle$ defining the geometric gate transformation^{60,61}

$$U(\Omega, \mathbf{n}) = e^{-i\Omega/2}|+\rangle\langle+| + e^{i\Omega/2}|-\rangle\langle-| = e^{-i\frac{1}{2}\Omega\mathbf{n}\cdot\boldsymbol{\sigma}}, \quad (27)$$

where $\boldsymbol{\sigma} = (\sigma_x, \sigma_y, \sigma_z)$ are the Pauli operators and $\mathbf{n} = (\sin\theta\cos\phi, \sin\theta\sin\phi, \cos\theta)$. Provided the solid angle and \mathbf{n} can be varied independently, $U(\Omega, \mathbf{n})$ is an arbitrary SU(2) transformation, i.e., a universal one-qubit gate.

The dynamical phase contributions of the $|\pm\rangle$ states can be eliminated either by employing refocusing technique^{63,64}, rotating driving fields with fine-tuned parameters^{60,61,65}, or by driving the qubit along geodesics on the Bloch sphere by using composite pulses⁶⁶. These techniques result in non-commuting gates solely dependent on the GPs of the cyclic states.

Physical implementation: NMR qubits

Quantum computation based on nuclear magnetic resonance (NMR) technique manipulates qubits encoded in nuclear spin- $\frac{1}{2}$. Such a qubit evolves due to the Zeeman interaction $\mu\mathbf{I}\cdot\mathbf{B}$, μ being the magnetic moment of the nuclei, \mathbf{I} the spin of the nuclei, and \mathbf{B} the applied magnetic field.

The nuclear spin states $|\uparrow; \mathbf{n}\rangle$ and $|\downarrow; \mathbf{n}\rangle$, \mathbf{n} being the quantization axis, acquire GPs $-\Omega/2$ and $+\Omega/2$, respectively, by adiabatically turning the magnetic field around a loop \mathcal{C} that starts and ends along \mathbf{n} and encloses the solid angle Ω . The dynamical phases are eliminated by refocusing, whereby the spin is taken around \mathcal{C} twice, the second time exactly retracing the first evolution but in opposite direction, and performing fast spin flips (π transformations) immediately before and after the second loop. Thus, the spin undergoes the evolution $\mathcal{C} \rightarrow \pi \rightarrow \mathcal{C}^{-1} \rightarrow \pi$. While the GPs of the qubit spin states $|\uparrow; \mathbf{n}\rangle$ and $|\downarrow; \mathbf{n}\rangle$ add up after performing the spin echo sequence, the dynamical phases exactly cancel leaving a purely geometric phase shift gate

$$U(2\Omega, \mathbf{n}) = e^{-i\Omega\mathbf{n}\cdot\boldsymbol{\sigma}}, \quad (28)$$

which is a universal one-qubit operation as noted above. A key point of the refocusing technique is that it makes the scheme insensitive to spatial variations of the magnetic field

strength so that all spin qubits in the sample undergo the same purely geometric transformation, determined by the same solid angle Ω swept by the direction of the slowly varying magnetic field⁶³.

Next, a conditional phase shift gate acting on two nuclear spin qubits can be realized by utilizing the standard NMR uniaxial spin-spin interaction $J I_{z;a} \otimes I_{z;b}$ in addition to the Zeeman term $(\mu_a \mathbf{I}_a + \mu_b \mathbf{I}_b) \cdot \mathbf{B}$ of the two spins a and b . The interaction term effectively shifts the z -component of the magnetic field by $J/(\mu_a + \mu_b)$ or $-J/(\mu_a + \mu_b)$ depending on whether the spins are parallel or anti-parallel. By choosing the initial quantization axis of the two spins along the z -direction, the sequence $\mathcal{C} \rightarrow \pi_a \rightarrow \mathcal{C}^{-1} \rightarrow \pi_b \rightarrow \mathcal{C} \rightarrow \pi_a \rightarrow \mathcal{C}^{-1} \rightarrow \pi_b$, where π_a and π_b are spin flips applied selectively to spins a and b , respectively, and \mathcal{C} is an adiabatic loop of the magnetic field, results in the conditional phase shift gate⁶³

$$\begin{aligned}
 U(\Delta\gamma) = & e^{2i\Delta\gamma} (|\uparrow_a \uparrow_b; z\rangle \langle \uparrow_a \uparrow_b; z| + |\downarrow_a \downarrow_b; z\rangle \langle \downarrow_a \downarrow_b; z|) \\
 & + e^{-2i\Delta\gamma} (|\uparrow_a \downarrow_b; z\rangle \langle \uparrow_a \downarrow_b; z| + |\downarrow_a \uparrow_b; z\rangle \langle \downarrow_a \uparrow_b; z|).
 \end{aligned}
 \tag{29}$$

Here,

$$\Delta\gamma = \gamma_+ - \gamma_-,
 \tag{30}$$

where $\gamma_{\pm} = \Omega_{\pm}/2$ with Ω_{\pm} being the solid angles enclosed by the effective magnetic fields $(B_x, B_y, B_z \pm J/(\mu_a + \mu_b))$.

Note that $U(\Delta\gamma)$ is entangling as it cannot be written as a product of unitary operators acting locally on each nuclear spin. Thus, $U(2\Omega, \mathbf{n})$ and $U(\Delta\gamma)$ form a universal set of one- and two-qubit gates that can be used to perform any quantum computation by purely geometric means.

Experiments

The conditional geometric phase shift gate $U(\Delta\gamma)$ has been demonstrated in NMR by Jones *et al.*⁶³. The two qubits were taken as the weakly interacting nuclear spins. The desired geometric gate was realized by adiabatically sweeping the magnetic field around a loop \mathcal{C} starting and ending along the z axis.

Another class of experiments related to GQC is based on the idea that the dynamical phase can in some cases be proportional to the geometric phase⁶⁷. This avoids the need

to eliminate the dynamical phase. Since such gates have non-zero dynamical phase, they are not geometric gates in a strict sense; nevertheless they share the potential robustness of standard geometric gates. The term ‘unconventional GQC’⁶⁷ has been coined for this type of gates.

In⁶⁸, a conditional π -phase two-qubit unconventional geometric gate combined with single-qubit rotations to produce a Bell state with 97% fidelity of two trapped ions has been demonstrated. A universal set of one- and two-qubit unconventional geometric gates with average fidelities 97-99% (one-qubit gates) and 93% (two-qubit gate) has been demonstrated in NMR⁶⁹. These high fidelities indicate the potential usefulness of Abelian geometric phases for robust quantum computation.

Holonomic quantum computation: GQC based on non-Abelian GPs

Non-Abelian GPs are matrix-valued and can therefore be non-commuting. By finding methods to eliminate the dynamical phases, all-geometric universal quantum computation can thus be implemented by using non-Abelian GPs.

In the standard scheme of non-Abelian GQC²⁵⁻²⁷, the dynamical phase is eliminated by utilizing adiabatic evolution of energetically degenerate subspaces. In this way, matrix-valued Wilczek-Zee phases¹⁸ are implemented that can be used to realize a universal set of quantum gates⁷⁰⁻⁷³. A difficulty in realizing these gates is the long run time associated with adiabatic evolution. In other words, adiabatic non-Abelian geometric gates operate slowly compared to the dynamical time scale, which make them vulnerable to open system effects and parameter fluctuations that may lead to loss of coherence.

To overcome the problem with the long run-time, GQC based on non-adiabatic non-Abelian GPs has been proposed⁶² and further developed⁷⁴⁻⁷⁶. The non-adiabatic scheme can be performed at high speed and involves less parameters to control experimentally than in the standard adiabatic scheme.

In the following, we describe the basic idea of adiabatic and non-adiabatic non-Abelian GQC. We describe the schemes in terms of trapped atoms or ions, which provide a versatile tool to perform quantum information processing by geometric means. Qubits encoded in the energy levels of the atoms or ions can be manipulated by external fields and the trapping

potential to realize universal non-adiabatic non-Abelian GPs.

Non-Abelian GQC: Adiabatic case

Adiabatic non-Abelian GQC can be implemented in an atomic or ionic system by controlling transitions between four energy levels by three independent laser pulses forming a tripod configuration. This scheme, first proposed for trapped ions or atoms^{70,71} (see also^{77,78}), and later for superconducting qubits⁷² and quantum dots⁷³, has become the standard one to perform GQC by means of adiabatic evolution. Other schemes not based on the tripod configuration can be found in^{79–82}.

The tripod shown in Figure 3, consists of four atomic or ionic energy levels $|0\rangle, |1\rangle, |a\rangle$ and $|e\rangle$ of the ‘bare’ Hamiltonian $H_0 = -\hbar(f_{e0}|0\rangle\langle 0| + f_{e1}|1\rangle\langle 1| + f_{ea}|a\rangle\langle a|)$ controlled by suitable external fields (by putting the ‘bare’ energy of the excited state to zero). The states $|0\rangle, |1\rangle, |a\rangle$ couple to the ‘excited’ state $|e\rangle$ by applying three oscillating electric field pulses $\mathbf{E}_j(t) = \epsilon_j g_j(t/T) \cos(f_j t)$, $j = 0, 1, a$, where the g_j ’s describe slowly varying shapes and relative phases of the pulses, and the ϵ_j ’s describe the polarization of the laser beams. By tuning the oscillation frequencies f_j so that detunings satisfy $f_j - f_{ej} \equiv \Delta$, the Hamiltonian in the interaction picture reads

$$H_I^{(1)}(t) = -\hbar\Delta|e\rangle\langle e| + \hbar(\omega_0(t/T)|e\rangle\langle 0| + \omega_1(t/T)|e\rangle\langle 1| + \omega_a(t/T)|e\rangle\langle a|) + \text{h.c.}, \quad (31)$$

where $\omega_j = \langle e|\boldsymbol{\mu} \cdot \boldsymbol{\epsilon}_j|j\rangle g_j/(2\hbar)$, $\boldsymbol{\mu}$ being the electric dipole moment operator, and we have neglected rapidly oscillating counter-rotating terms $e^{\pm 2if_{ej}t}$ terms (rotating wave approximation (RWA)).

The interaction Hamiltonian $H_I^{(1)}(t)$ has two degenerate dark energy eigenstates:

$$\begin{aligned} |D_1; \theta, \phi\rangle &= -\sin\varphi e^{i(S_3-S_1)}|0\rangle + \cos\varphi e^{i(S_3-S_2)}|1\rangle, \\ |D_2; \theta, \phi\rangle &= \cos\vartheta (\cos\varphi e^{i(S_3-S_1)}|0\rangle + \sin\varphi e^{i(S_3-S_2)}|1\rangle) - \sin\vartheta|a\rangle, \end{aligned} \quad (32)$$

where $\omega_0 = \omega \sin\vartheta \cos\varphi e^{iS_1}$, $\omega_1 = \omega \sin\vartheta \sin\varphi e^{iS_2}$, and $\omega_a = \omega \cos\vartheta e^{iS_3}$. These dark eigenstates coincide with the realization of the non-commuting one-qubit operations $U[\mathcal{C}_1]$ and $U[\mathcal{C}_2]$ in Eqs. (24) and (26) by identifying the adiabatic parameters $(\vartheta, \varphi, S_3 - S_1, S_3 - S_2)$ with $(\kappa/2, \pi/2, 0, -\eta)$ and $(\kappa, \eta, 0, 0)$, respectively. These two gates are realized by varying the parameters κ, η in the $T \rightarrow \infty$ adiabatic limit.

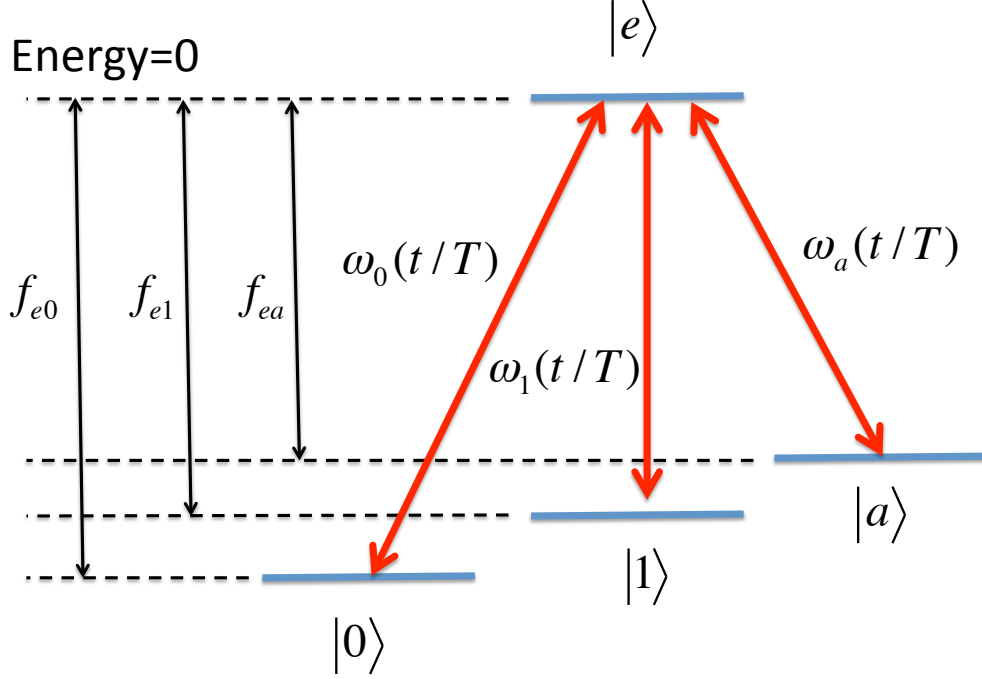


Figure 2: Tripod setting consisting of three energy levels $|0\rangle$, $|1\rangle$, and $|a\rangle$ coupled to an excited state $|e\rangle$ at zero energy by laser pulses with the same detuning. Adiabatic non-Abelian geometric gates can be implemented by slowly varying the complex-valued laser parameters ω_j , $j = 0, 1, a$, around a loop in parameter space. The parameters start and end so that the two-dimensional dark subspace coincide with the qubit subspace $\text{Span}\{|0\rangle, |1\rangle\}$.

The above $U[\mathcal{C}_1]$ and $U[\mathcal{C}_2]$ form a universal set together with any entangling geometric two-qubit gate. For trapped ions, such a gate can be performed by utilizing the Sørensen-Mølmer setting⁸³, resulting in the Hamiltonian⁷⁰

$$H_I^{(2)}(t) = \omega \left(-\sin \frac{\kappa}{2} e^{i\eta} |ee\rangle \langle 11| + \cos \frac{\kappa}{2} |ee\rangle \langle aa| + \text{h.c.} \right), \quad (33)$$

which has a single dark state $|D; \kappa, \eta\rangle = \cos \frac{\kappa}{2} |11\rangle + e^{i\eta} \sin \frac{\kappa}{2} |aa\rangle$ that picks up the GP

$$U[\mathcal{C}_3] = e^{-i|11\rangle \langle 11| \oint (1 - \cos \kappa) d\eta} \quad (34)$$

by adiabatically changing κ and η around a loop in parameter space. $U[\mathcal{C}_1]$, $U[\mathcal{C}_2]$, and $U[\mathcal{C}_3]$

form a universal set of geometric quantum gates that can be used to build any quantum computation by purely geometric means.

Non-Abelian GQC: Non-adiabatic case

Non-adiabatic non-Abelian GQC⁶² in an atomic or ionic system requires control of three energy levels by suitable external laser fields forming a Λ -system. By following the same procedure as above, we obtain the Hamiltonian

$$H_I^{(1)}(t) = \omega_0(t)|e\rangle\langle 0| + \omega_1(t)|e\rangle\langle 1| + \text{h.c.} \quad (35)$$

by employing the RWA in the interaction picture and by requiring zero detuning. A key difference compared to the adiabatic scheme is that the complex-valued Rabi frequencies $\omega_0(t), \omega_1(t)$ are allowed to be varied at any speed.

A non-Abelian geometric one-qubit gate $U[\mathcal{C}]$ acting on the qubit subspace is implemented by choosing laser field pulses of duration τ such that $\omega_0(t)/\omega_1(t) \equiv -\tan(\theta/2)e^{i\phi}$ is time independent and satisfy the criterion $\int_0^\tau \sqrt{|\omega_0(t)|^2 + |\omega_1(t)|^2} dt = \pi$. Here, the latter condition assures that the qubit subspace $\text{Span}\{|0\rangle, |1\rangle\}$ undergoes a cyclic evolution defining a loop \mathcal{C} in the space of two-dimensional subspaces of the three-dimensional Hilbert space $\text{Span}\{|0\rangle, |1\rangle, |e\rangle\}$; the former guarantees that the dynamical phases vanish for the full pulse duration, which implies that the gate is fully determined by \mathcal{C} . Explicitly,

$$U[\mathcal{C}] = \mathbf{n} \cdot \boldsymbol{\sigma}, \quad (36)$$

where $\boldsymbol{\sigma}$ are the Pauli operators acting on the qubit subspace. This unitary corresponds to a 180° rotation of the qubit around the ‘direction’ $\mathbf{n} = (\sin \theta \cos \phi, \sin \theta \sin \phi, \cos \theta)$ defined by relative phase and amplitude of the pair of laser fields. Performing sequentially two such gates with different laser parameters defining directions \mathbf{n} and \mathbf{n}' yields

$$U(\mathcal{C}')U[\mathcal{C}] = \mathbf{n}' \cdot \mathbf{n} + i\boldsymbol{\sigma} \cdot (\mathbf{n}' \times \mathbf{n}), \quad (37)$$

which is an arbitrary $\text{SU}(2)$ operation, i.e., a universal one-qubit gate. Geometrically, the gate can be visualized as a rotation of the qubit by an angle $-2 \arccos(\mathbf{n}' \cdot \mathbf{n})$ around the direction $\mathbf{n}' \times \mathbf{n}$.

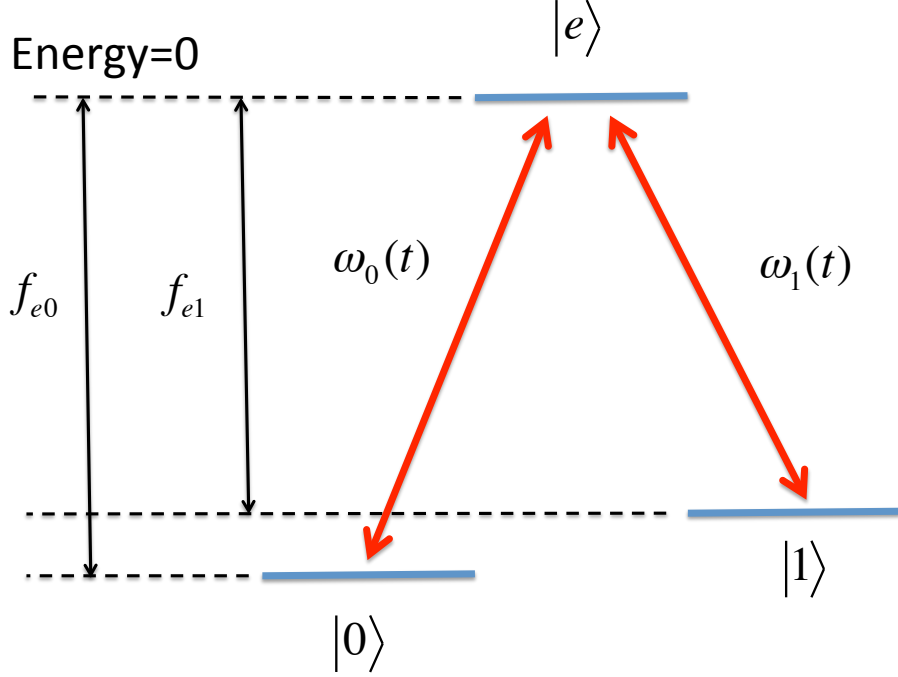


Figure 3: A setting consisting of two energy levels $|0\rangle$ and $|1\rangle$ coupled to an excited state $|e\rangle$ at zero energy by a pair of zero-detuned laser pulses. Non-adiabatic non-Abelian geometric gates acting on a qubit encoded in the subspace $\text{Span}\{|0\rangle, |1\rangle\}$ can be implemented by varying the complex-valued laser parameters ω_j , $j = 0, 1, a$, but keeping $\omega_0(t)/\omega_1(t)$ constant over each pulse pair chosen to satisfy the π pulse criterion $\int_0^\tau \sqrt{|\omega_0(t)|^2 + |\omega_1(t)|^2} dt = \pi$.

Similar to the adiabatic realization, the universal set is completed by adding a geometric two-qubit gate in the Sørensen-Mølmer setting⁸³. The differences are that each ion needs to exhibit only an internal three-level structure $|0\rangle$, $|1\rangle$ and $|e\rangle$, and the amplitude ratio $\tan(\theta/2)$ as well as the phase shift ϕ of two laser beams should be kept constant during each pulse pair. The resulting Hamiltonian acting on the computational subspace $\{|00\rangle, |01\rangle, |10\rangle, |11\rangle\}$ reads

$$H_I^{(2)} = \omega(t) \left(\sin \frac{\theta}{2} e^{i\phi/2} |ee\rangle\langle 00| - \cos \frac{\theta}{2} e^{-i\phi/2} |ee\rangle\langle 11| + \text{h.c.} \right). \quad (38)$$

The π pulse criterion $\int_0^\tau \omega(t)dt = \pi$ results in the geometric two-qubit gate

$$\begin{aligned}
U[\mathcal{C}] = & \cos \theta |00\rangle\langle 00| + \sin \theta e^{-i\phi} |00\rangle\langle 11| \\
& + \sin \theta e^{i\phi} |11\rangle\langle 00| - \cos \theta |11\rangle\langle 11| \\
& + |01\rangle\langle 01| + |10\rangle\langle 10|.
\end{aligned} \tag{39}$$

The path \mathcal{C} , being characterized by the unit vector $\mathbf{n} = (\sin \theta \cos \phi, \sin \theta \sin \phi, \cos \theta)$ in \mathbb{R}^3 , is traversed in the three dimensional subspace spanned by $\{|00\rangle, |11\rangle, |ee\rangle\}$ of the internal degrees of freedom of the ions. Note that $U[\mathcal{C}]$ is entangling as it cannot be written as a product of unitary operators acting locally on each ion qubit. It completes the universal set of non-adiabatic non-Abelian geometric gates that can be used to perform fast quantum computation by purely geometric means.

Experiments

The scheme for non-adiabatic GQC proposed in⁶² has been realized in several recent experiments⁸⁴⁻⁸⁷. Non-commuting operations in a superconducting transmon one-qubit system have been demonstrated⁸⁴. A universal set of one- and two-qubit non-Abelian geometric gates has been implemented⁸⁵ in a liquid state NMR quantum information processor using a three-qubit variant of⁶² akin to⁸⁸.

To achieve GQC at room temperature in a naturally scalable system, spin qubits associated with a nitrogen-vacancy color centre in diamond have been used^{86,87}. While⁸⁶ was limited to one-qubit operations, the full universal set of quantum gates, including a universal CNOT gate, which is $\text{CNOT}|x\rangle \otimes |y\rangle = |x\rangle \otimes |x \oplus y\rangle$ (\oplus is addition mod 2 and x, y take values 0 or 1), has been implemented⁸⁷. This CNOT gate applied to an initial product state has been shown to yield a concurrence⁸⁹ of 0.85, which unambiguously confirmed its entangling nature.

A recent experiment⁹⁰ has demonstrated GQC using adiabatic evolution in a tripod configuration, where three ground state levels couple to an excited state by use of three resonant laser fields. This experiment realized a universal set of one-qubit gates based on the adiabatic scheme proposed in⁷⁰ resulting from adiabatic transport of this dark energy eigensubspace for a single trapped ion.

Robustness of GQC

A key motivation for GQC is the potential robustness of GPs to errors, such as decoherence and parameter noise²⁷. To examine the validity of this conjecture, several studies have been carried out, testing the behavior of different forms of GQC to different kinds of errors. We summarize a few of these as follows:

- To address the question whether geometric gates are more robust than dynamical gates, Zhu and Zanardi⁶⁵ have designed a scheme where the two types of gates can be continuously changed into each other. The basic idea is to implement a one-qubit phase shift gates $U(\gamma) = e^{i\gamma}|+\rangle\langle+| + e^{-i\gamma}|-\rangle\langle-|$ by exposing the qubit to a rotating magnetic field. By suitably changing the frequency and opening angle of the magnetic field, γ can be varied from a purely dynamical phase δ to a purely geometric phase $\Phi[\mathcal{C}]$. The optimal fidelity under parameter noise is obtained for a purely geometric gate. Although this result provides evidence for the advantage of GQC with regard to resilience to dephasing errors in this setting, there are other settings where the geometric approach seems to have no particular advantage compared to a dynamical approach when considering certain decoherence⁹¹ and parameter noise⁹² models.
- The conditional two-qubit geometric phase gate in Eq. (29) exhibits optimal parameter values, where $\Delta\gamma$ is resilient to errors in the amplitude of the RF field⁶⁴. Similar optimal working points have been found at certain run-times in finite time realization of non-Abelian GQC under influence of an oscillator bath^{93,94} and parameter noise⁹⁵.
- The robustness of adiabatic and non-adiabatic realizations of non-Abelian GQC to parameter errors, decay, and dephasing have been examined⁹⁶. The adiabatic gates are robust to decay and mean detuning error in the large run-time limit, but they are highly sensitive to dephasing and relative detuning error in this limit. The non-adiabatic gates, on the other hand, become resilient to all these imperfections by employing pulses that are sufficiently short. However, there is a limit for how short the pulses can be before RWA breaks down. In fact, the experiment in⁸⁴ did use pulse lengths close to this limit. Thus, one can predict that further speed-up in this setup would lead to highly unstable gates⁹⁷.

- Corrections to the GP of a spin- $\frac{1}{2}$ in the adiabatic $T \rightarrow \infty$ limit have been found to decay as $1/T$, while the corrections to the dynamical phase grows as T , by assuming a physically reasonable parameter noise model⁹⁸. This effect has been studied experimentally for microwave-driven superconducting qubits^{99,100} and trapped polarized ultracold neutrons¹⁰¹.
- Robustness can be improved by combining GQC with other error resilient schemes. Adiabatic non-Abelian GQC have been combined¹⁰² (see also^{103–106}) with the theory of decoherence free subspaces (DFSs)^{107,108} and noiseless subsystems¹⁰⁹. This idea has been generalized to the non-adiabatic case^{88,110}. It has further been proved that GQC is scalable under a reasonable noise model by combining it with fault tolerant quantum error correction^{111,112}. All these approaches are experimentally challenging since they requires 3- or 4-body terms in the underlying Hamiltonian, while only 2-body terms occur naturally in nature. This problem may be addressed by using perturbative gadgets¹¹³ to simulate many-body interactions. An alternative solution is the recent proposal¹¹⁴ to combine the Zhu-Wang approach to Abelian GQC^{60,61} and the theory of DFSs, which removes the need for many-body terms but retains the universality of the geometric scheme. Finally, non-adiabatic GQC has been combined with dynamical decoupling¹¹⁵, i.e., the idea to average out the effect of noise by fine-tuned spin flipping¹¹⁶.

MIXED STATES

The concept of pure quantum states is an idealization. In experiments, mixtures of pure states arise naturally due to inevitable imperfections in the preparation procedure and open system effects during evolution. Therefore, a more realistic description of experiments requires the notion of mixed quantum states.

The mathematical representation of mixed states is given by density operators, which are linear operators ρ satisfying $\rho \geq 0$ and $\text{Tr}\rho = 1$. For a mixture of pure states $\{\psi_j\}$ occurring with relative frequencies $\{p_j\}$, one can write $\rho = \sum_j p_j |\psi_j\rangle\langle\psi_j|$, which explicitly entails the relation between the mixture $\{p_j, \psi_j\}$ and its mathematical representation ρ . The density

operator contains all empirically available information in the sense that it can be used to fully predict probabilities of outcomes in any conceivable experiment on a given quantum system.

Now, to examine the robustness of GQC under influence of open system effects as well as imprecise preparation, we need to understand the meaning of GP associated with evolution of mixed quantum states. The basic question is, in other words, how to associate a physically meaningful GP to a path $t \in [0, \tau] \rightarrow \rho(t)$ of mixed states. For closed system evolution, such a path is a continuous one-parameter family of unitary transformations of the input density operator $\rho(0)$, i.e., $\rho(t) = U(t)\rho(0)U^\dagger(t)$; for an open system the evolution takes the form $\rho(t) = e^{\int_0^t \mathcal{L}(t')dt'} \rho(0)$, where \mathcal{L} is a superoperator. For instance, in the Markovian limit case, \mathcal{L} takes the Lindblad form¹¹⁷ $\mathcal{L}(t)\rho = -(i/\hbar)[H(t), \rho] + \sum_k \left(L_k \rho L_k^\dagger - (1/2)\{\rho, L_k^\dagger L_k\} \right)$, where the Lindblad operators L_k are arbitrary linear operators and $[\cdot, \cdot]$ ($\{\cdot, \cdot\}$) is the commutator (anti-commutator).

There are two main forms of GP for mixed states:

- (i) GP based on interferometry²⁹. Here, the idea is to start from a Mach-Zehnder setup shown in Figure 4, where an incoming beam carrying an internal state ρ (spin, say) is split by a 50-50 beam-splitter, the beam-pair brought together by two mirrors to finally interfere at a second 50-50 beam-splitter. The internal state ρ is assumed to be unaffected by the beam-splitters and mirrors. By exposing one of the beams to a unitary U , acting on the internal state ρ , and the other beam to a $U(1)$ phase shift $e^{i\chi}$, we obtain the output intensity

$$I \propto 1 + |\text{Tr}(\rho U)| \cos[\chi - \arg \text{Tr}(\rho U)] \quad (40)$$

in one of the output beams. Thus, the interference oscillations produced by varying χ is characterized by the phase shift $\arg \text{Tr}(\rho U)$ and visibility $|\text{Tr}(\rho U)|$. The shift $\arg \text{Tr}(\rho U)$ is the Pancharatnam relative phase^{21,29} acquired by the internal state ρ exposed to a unitary U .

To see how this setting can be used to define a geometric phase associated with the unitary path $\mathcal{C} : t \in [0, \tau] \rightarrow U(t)\rho U^\dagger(t)$, we use the spectral decomposition of the

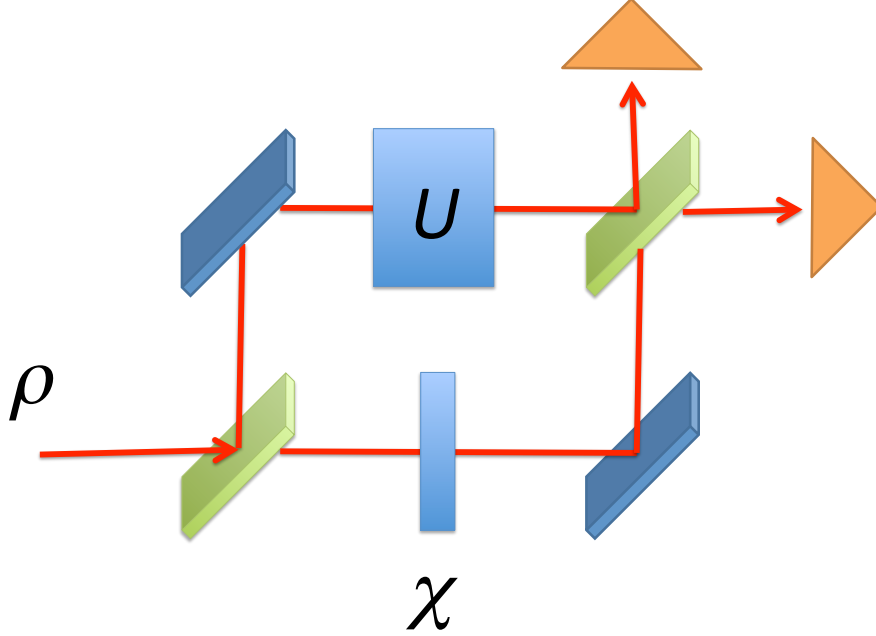


Figure 4: Mach-Zehnder interferometer setup to measure the Pancharatnam relative phase $\arg \text{Tr}(\rho U)$ acquired by an internal state ρ exposed to a unitary U in the upper beam. The phase is measured as a shift in the interference oscillations in one of the output beams obtained by varying the U(1) shift χ in the lower beam.

density operator, i.e., $\rho = \sum p_n |n\rangle\langle n|$ with p_n being time-independent probabilities of the orthonormal eigenstates $|n\rangle$ of ρ . We obtain

$$\text{Tr}[\rho U(\tau)] = \sum_{n=1}^N p_n \langle n|U(\tau)|n\rangle = \sum_{n=1}^N p_n |\langle n|U(\tau)|n\rangle| e^{if_n}, \quad (41)$$

f_n being the global phase acquired by the eigenstate $|n\rangle$ under the evolution and N being the dimension of the system's Hilbert space. Each such global phase contain a geometric part $\arg\langle n|U(\tau)|n\rangle + i \int_0^\tau \langle n|U^\dagger(t)\dot{U}(t)|n\rangle dt$ and a dynamical part $-i \int_0^\tau \langle n|U^\dagger(t)\dot{U}(t)|n\rangle dt$. By demanding parallel transport of each such eigenstate, we obtain the geometric phase shift²⁹

$$\Phi[\mathcal{C}] = \arg \sum_{n=1}^N p_n \langle n|U(\tau)|n\rangle e^{i \int_0^\tau \langle n|U^\dagger(t)\dot{U}(t)|n\rangle dt}, \quad (42)$$

thus the GP factor $e^{i\Phi[\mathcal{C}]}$ is the weighted sum of GP factors of the eigenstates of ρ with weights $p_n |\langle n|U(\tau)|n\rangle|$. This GP is experimentally accessible since there are exactly

N independent phase factors $\{e^{i\alpha_n(t)}\}_{n=1}^N$ that are not determined by the evolution, as can be seen by noting that the $U(t)\rho U^\dagger(t)$ is unchanged under the transformation $U(t) \rightarrow U(t) \sum_{n=1}^N e^{i\alpha_n(t)} |n\rangle\langle n|$. These phase factors can be used to realize parallel transport of each eigenstate of the density operator.

Provided ρ is non-degenerate, $\Phi[\mathcal{C}]$ in Eq. (42) is a unique concept of GP. For a degenerate eigenvalue, however, the corresponding eigenstates are not uniquely given and therefore the above definition does not provide a unique GP. The generalization to degenerate density operators has therefore been carried out¹¹⁸, based on the idea that the degenerate subspace(s) can be associated non-Abelian GPs in the same vein as in the Wilczek-Zee¹⁸ and Anandan²⁰ approaches.

The mixed state GP in²⁹ has been generalized and to arbitrary open system evolution³⁰ (for some applications, see^{119–122}), for which the probabilities of the spectral decomposition are generically time-dependent, i.e., $\rho(t) = \sum_{n=1}^N p_n(t) |\psi_n(t)\rangle\langle\psi_n(t)|$ with $\langle\psi_n(t)|\psi_m(t)\rangle = \delta_{nm}$. The natural generalization of Eq. (42) is³⁰

$$\Phi[\mathcal{C}] = \arg \sum_{n=1}^N \sqrt{p_n(0)p_n(\tau)} \langle\psi_n(0)|\psi_n(\tau)\rangle e^{i \int_0^\tau \langle\psi_n(t)|\dot{\psi}_n(t)\rangle dt}, \quad (43)$$

where the square root of the initial and final probabilities is a consequence of Schmidt-form purification $\rho(t) \rightarrow \sum_{n=1}^N \sqrt{p_n(t)} |\psi_n(t)\rangle|a_n\rangle$, where $\{|a_n\rangle\}$ is a fixed orthonormal ancilla basis.

- (ii) The Uhlmann GP^{28,123,124}. This is a non-Abelian GP of mixed quantum states based on purification, i.e., the idea that any density operator can be written as the partial trace of a pure state of a larger system consisting of the considered system and an ancilla. This GP is defined via a parallelity condition that singles out a preferred purification of a density operator ρ_{k+1} given a purification of another density operator ρ_k . Explicitly, a purification of a density operator ρ is a mapping $\rho \rightarrow |\psi_\rho\rangle = \sum_{n=1}^N (\sqrt{\rho} |e_n\rangle) \otimes V^T |e_n\rangle$, V being an arbitrary unitary with T transposition with respect to the fixed orthonormal basis $|e_n\rangle$. Parallelity is defined as

$$\max_{V_{k+1}} |\langle\psi_{\rho_{k+1}}|\psi_{\rho_k}\rangle| = \text{Tr} \sqrt{\sqrt{\rho_k} \rho_{k+1} \sqrt{\rho_k}} \quad (44)$$

where the right-hand side is the Uhlmann fidelity¹²⁵ that measures the similarity of the two states ρ_k and ρ_{k+1} . The optimal purification is given by the unitary

$$V_{k+1} = V_{\rho_{k+1}\rho_k} V_k, \quad (45)$$

where $V_{\rho_{k+1}\rho_k}$ is the unitary part of $\sqrt{\rho_{k+1}}\sqrt{\rho_k}$. Here, $V_{\rho_{k+1}\rho_k}$ is a unique unitary provided the density operators are both full rank. The lower rank cases, such as the pure state case, must be treated separately; in these cases the relative phases become partial isometries. By repeating this argument along a sequence $\mathcal{C} : \rho_1, \dots, \rho_K$ we obtain the Uhlmann GP

$$U[\mathcal{C}] = V_{\rho_K\rho_{K-1}} \cdots V_{\rho_2\rho_1} V_1^\dagger, \quad (46)$$

where the multiplication with V_1^\dagger from the right removes the arbitrary choice of initial purification, and makes the resulting unitary operator $U[\mathcal{C}]$ gauge invariant. The Uhlmann scheme can be applied to any continuous rank-preserving path by taking appropriate limit of the right-hand side of Eq. (46).

One may notice that the above scheme is of rather mathematical nature and its physical meaning might seem a bit unclear. Nevertheless, it has been pointed out that it can in principle be realized interferometrically, provided the ancilla system can be fully controlled^{126,127}. Recent work have further shown the usefulness of the Uhlmann GP to analyze temperature effects in topological states of matter^{128–130}.

We have seen that there are two different routes to define a GP for mixed quantum states. A natural question then arise: are the resulting phases in some way related? Various aspects of this issue have been addressed. First, it has been shown that the Uhlmann and interferometer GPs are indeed distinct concepts that only fully coincide in the special case of pure states^{126,131}. The key difference lies in that while the interferometer based GP can be measured in a single-particle interference the Uhlmann GP is a property of a larger system in the sense that it can only be measured in two-particle interference^{126,127}. Further, the question as to whether the two mixed state GPs arise out of a single more fundamental notion of GP for mixed states has been addressed^{132–134}.

Physical example: Unitary evolution of a qubit

We illustrate the two GP concepts for mixed states in the case of unitary evolution of a single qubit. Any qubit density operators can be written as

$$\rho = \frac{1}{2} (\hat{1} + \mathbf{r} \cdot \boldsymbol{\sigma}), \quad (47)$$

where $\hat{1}$ is the identity operator and the Bloch vector $\mathbf{r} = (x, y, z)$ satisfies $|\mathbf{r}| \leq 1$, with equality if and only if ρ is a pure state. Thus, the pure states reside on the two-dimensional Bloch sphere and the non-pure states are in the interior of this sphere. In particular, the origin $\mathbf{r} = 0$ corresponds to a equally weighed mixture of any orthogonal states (random mixture).

Let us first consider the interferometric approach. Let the eigenstates of ρ be $|\pm\rangle$ with eigenvalues $\frac{1}{2}(1 \pm r)$, $r = |\mathbf{r}|$. Assume that the qubit undergoes cyclic unitary evolution such that the Bloch vector \mathbf{r} traces out a path \mathcal{C} that encloses a solid angle Ω . It follows that $|\langle \pm | U(\tau) | \pm \rangle| = 1$ and

$$|\text{Tr}(\rho U(\tau))| e^{i\Phi[\mathcal{C}]} = \frac{1+r}{2} e^{-i\Omega/2} + \frac{1-r}{2} e^{i\Omega/2}, \quad (48)$$

which yields

$$\begin{aligned} \Phi[\mathcal{C}] &= -\arctan\left(r \tan \frac{\Omega}{2}\right), \\ |\text{Tr}(\rho U(\tau))| &= \sqrt{\cos^2 \frac{\Omega}{2} + r^2 \sin^2 \frac{\Omega}{2}}, \end{aligned} \quad (49)$$

where the first expression gives the mixed state GP and the second is the visibility of the interference fringes that would be detected in an interferometer setting. Both these quantities are determined by the enclosed solid angle Ω on the Bloch sphere and the degree of mixing r ; they reduce to the expected expressions $\Phi[\mathcal{C}] = -\Omega/2$ and $|\text{Tr}(\rho U(\tau))| = 1$ in the pure state limit $r \rightarrow 1$. Note that the density operator is degenerate in the limit of random mixtures $r \rightarrow 0$, which implies that there is no unique eigenbasis of ρ and the mixed state GP becomes undefined. Subtle interference effects close to this singularity have been examined^{135,136}.

Let us now turn to the Uhlmann GP. This GP is a non-Abelian quantity, which mean that it involves a time ordered product or integral. To deal with this complication, one may

restrict to specific paths in state space. Here, we consider unitary evolution of the qubit around a great circle \mathcal{G} inside the Bloch sphere chosen to start and end at the positive z axis and restricted to the xz plane. Such paths play a natural role to study temperature-driven phase transitions of the Uhlmann GP of fermion systems^{128–130}. We find

$$U[\mathcal{G}] = -e^{i\sqrt{1-r^2}\pi\sigma_y}. \quad (50)$$

In the limit of random mixtures $r \rightarrow 0$, the Uhlmann GP is still well-defined but trivial, i.e., $U[\mathcal{G}] = \hat{1}$. The pure state limit $r \rightarrow 1$, on the other hand, is more subtle. In this limit, ρ has rank 1 and $U[\mathcal{G}]$ should be interpreted as a $U(1)$ phase factor times a projector. Explicitly, one finds

$$U[\mathcal{G}] = -|+\rangle\langle+|, \quad (51)$$

where the minus sign coincides with the expected pure state GP of π associated with a great circle on the Bloch sphere.

Measurement of mixed state GPs

Direct experimental tests of the mixed state GP²⁹ by using interferometry techniques have been carried out in NMR systems^{137,138}. These experiments utilize two nuclear spin- $\frac{1}{2}$ with one spin playing the role of the interferometer arms while implementing the unitary geometric transformation on the second spin, conditionally on the state of the first spin. The dependence of $\Phi[\mathcal{C}]$ in Eq. (49) on the degree of mixing r has been verified^{137,138}, as well as the r and Ω dependence of the visibility¹³⁸. A related NMR experiment¹³⁹ has examined the mixed state GP proposed in³⁰ for non-unitary evolution.

Experimental test of²⁹ has been performed by using polarization mixed states of photons in a Mach-Zehnder interferometer setup¹⁴⁰. These polarization states were prepared in two different ways, either by using birefringent decoherers that couple the single photon's polarization to its arrival time relative to the trigger or by preparing non-maximally polarization-entangled photon pairs and measuring the phase of one of the photons while tracing over the other. These two cases correspond to two types of mixed states, proper and

improper ones¹⁴¹, where the latter concept refers to that the state of the full system is in fact pure.

In addition to interferometry, quantum mechanical phase shifts can as well be performed using single-beam polarimetric techniques. The basic setting to perform such experiments has been developed⁵⁰ and later generalized to mixed states¹⁴². The latter has been realized in a single-beam experiment on partially polarized neutrons¹⁴³ and utilized to test the non-additive nature of phase shifts (geometric or dynamical) for mixed quantum states¹⁴⁴.

Due to the high-level of control required, the Uhlmann GP is considerably more challenging to implement experimentally. Nevertheless, it has been measured by using NMR technique for a qubit undergoing unitary evolution and comparing it with the interferometric GP for the same paths in the space of density operators¹⁴⁵. The measured phases were explicitly shown to behave differently, providing clear experimental evidence of the inequivalence of the interferometer-based and Uhlmann GPs.

ENTANGLEMENT

Entanglement is fundamental resource in quantum information that can be used for secure key distribution¹⁴⁶, teleportation¹⁴⁷, and information processing¹⁴⁸. The most basic form of entanglement is given by the four Bell states, which form the orthogonal basis states

$$\begin{aligned} |\Phi_{\pm}\rangle &= \frac{1}{\sqrt{2}}(|00\rangle \pm |11\rangle), \\ |\Psi_{\pm}\rangle &= \frac{1}{\sqrt{2}}(|01\rangle \pm |10\rangle) \end{aligned} \quad (52)$$

of two qubits. These are maximally entangled in the sense that each of them contains full information about the two qubits, but completely random information for each qubit separately.

The concept of entanglement becomes even richer when considering more than two qubits. The additional richness lies in the fact that while two qubits essentially can be entangled in only one way (given by the above Bell state entanglement), there are several ways to entangle three or more qubits. To analyze this structure, it is convenient to use the concept of stochastic local operations and classical communication (SLOCC), i.e., the idea that entan-

glement cannot be changed if only local operations (unitary, measurements, etc) and classical communication are allowed. In this language, one may for instance show that three-qubit system in pure states can entangle in two different ways, in the sense that a state picked from one of these two classes cannot be taken to a state in the other class by performing SLOCC¹⁴⁹. The two classes, called W and GHZ, have their basic forms

$$\begin{aligned} |W\rangle &= a|001\rangle + b|010\rangle + c|100\rangle, \\ |\text{GHZ}\rangle &= a'|000\rangle + b'|111\rangle, \end{aligned} \tag{53}$$

where the first is characterized by two-qubit entanglement only, while the second is genuinely three-qubit entangled but with no two-qubit entanglement¹⁵⁰.

Entanglement can be quantified by using various kinds of measures, such as entanglement of formation¹⁵¹, geometric entanglement^{152,153}, and relative entropy of entanglement¹⁵⁴. Besides quantification of its amount, entanglement can be characterized qualitatively by using suitable polynomials of the expansion coefficients with respect to a product basis spanning the composite system's Hilbert space. For two qubits in the state $\sum_{kl} \alpha_{kl} |kl\rangle$, $\det[\alpha_{kl}] = \alpha_{00}\alpha_{11} - \alpha_{01}\alpha_{10}$ is a polynomial invariant under SLOCC and therefore a property of entanglement. Furthermore, this degree-2 polynomial determines the entanglement of formation via the concurrence measure⁸⁹ $C = 2|\det[\alpha_{kl}]|$. Similarly, the hyperdeterminant of the expansion coefficients α_{klm} of a pure three-qubit state is a SLOCC invariant degree-4 polynomial that determines the 3-tangle, one of the main measures of three-qubit entanglement¹⁵⁰. The characterization in terms of invariant polynomials becomes increasingly complicated when the number of subsystems increases^{155,156}.

In the following, we focus on a type of topological phases for entangled systems undergoing local special unitary (SU) evolution; a subclass of SLOCC operations. These topological phases were first discovered for two-qubit systems^{45,157–159}, and later generalized to qudit (d -level) pairs^{46,160,161} and to multi-qubit systems⁴⁷. They may in some cases coincide with the corresponding GPs. We delineate the relation between the topological phases and local SU invariant polynomials and describe experimental work to study these phases. The key merit of the entanglement-induced topological phases is that they constitute a novel perspective that may provide further insights into the nature of quantum entanglement.

A non-exhaustive list of other studies of GP effects in entangled systems is as follows. GPs of bipartite qubit systems in pure states have been examined^{162–164} in terms of the concept of ‘Schmidt sphere’¹⁶², built on the analogy of the Bloch sphere of a single qubit, and by use of properties of braiding transformations to represent entangled two-qubit states¹⁶⁴. Recently, the Schmidt sphere concept has been examined in a quantum optical experiment¹⁶⁵. The relation between the GPs of an entangled system and its subsystems has been examined^{166,167}. GP effects have been shown to play a role for the understanding of entanglement in multi-particle systems^{168–170}. GPs for sequences of relative states, obtained by projecting on one subsystem of a bipartite composite system, have been studied for pure¹⁷¹ and mixed¹⁷² states. GPs associated with spin-orbit entanglement in neutron interferometry have been predicted¹⁷³ and experimentally observed¹⁷⁴. A relation between the GP of a two-qubit state and concurrence has been delineated¹⁷⁵. Pure two-qubit states can be represented as single-qubit states with quaternionic expansion coefficients¹⁷⁶. The non-Abelian and entanglement-dependent GPs associated with this quaternionic representation have been examined^{177,178}.

Topological phases of entangled systems: bipartite case

Let us first consider the case of maximally entangled states (MES) of pairs of qubits. Any such state can be written on the form

$$|a, b\rangle = \frac{1}{\sqrt{2}} \left(a|00\rangle + b|01\rangle - b^*|10\rangle + a^*|11\rangle \right), \quad (54)$$

where a and b are arbitrary complex numbers with $|a|^2 + |b|^2 = 1$. The four Bell states in Eq. (52) correspond to the choices $(a, b) = (1, 0), (i, 0), (0, i)$, and $(0, 1)$, respectively. These states can be transformed into each other by applying local $SU(2)$ transformations U and V . The states of the single qubit subsystems A and B are given by the reduced density operators ρ_A and ρ_B obtained by tracing over qubit B and A , respectively. For the MES $|a, b\rangle$, the reduced density operators take the form $\frac{1}{2}\hat{1}_A$ and $\frac{1}{2}\hat{1}_B$, irrespective of the values of a and b . Thus, the subsystem states correspond to random mixtures for all MES.

We are interested in continuous paths $\mathcal{C} : t \in [0, \tau] \rightarrow (a(t), b(t))$ corresponding to the pure state local unitary evolution $|a(0), b(0)\rangle \rightarrow |a(t), b(t)\rangle = U(t) \otimes V(t)|a(0), b(0)\rangle$, such that the state traces out a loop in state space of the qubit-pair, i.e., $|a(\tau), b(\tau)\rangle =$

$e^{if}|a(0), b(0)\rangle$. We can now observe two important features of this evolution:

- In order to preserve the MES form in Eq. (54), f can only take one of two values, namely, 0 or π .
- The accumulation of local phase changes

$$i \int_0^\tau \langle a(t), b(t) | \frac{d}{dt} |a(t), b(t)\rangle dt = i \int_0^\tau \text{Tr} \left(\frac{1}{2} \hat{1}_A U^\dagger \dot{U} \right) dt + i \int_0^\tau \text{Tr} \left(\frac{1}{2} \hat{1}_B V^\dagger \dot{V} \right) dt \quad (55)$$

vanishes, since the infinitesimal generators $U^\dagger \dot{U}$ and $V^\dagger \dot{V}$ of $U, V \in \text{SU}(2)$ are traceless.

The first feature demonstrates the topological nature of the acquired phase f : it is impossible to transform between the two allowed values 0 and π by continuously deforming the path \mathcal{C} . In fact, the two phases can be associated with the doubly-connectedness of $\text{SO}(3)$. This may be seen by noting that the state space of MES is given by

$$\text{MES} \simeq \{(a, b) \in C^2 \text{ such that } |a|^2 + |b|^2 = 1 \text{ and } (a, b) \sim (-a, -b)\}. \quad (56)$$

This shows that there is a one-to-one correspondence between MES and the three-dimensional sphere S^3 ($|a|^2 + |b|^2 = 1$) with antipodal points identified ($(a, b) \sim (-a, -b)$), which is isomorphic to the three-dimensional rotation group $\text{SO}(3)$, i.e., $S^3/Z_2 \simeq \text{SO}(3)$. Now, $\text{SO}(3)$ is known to be doubly-connected, which means that there are two types of topologically inequivalent loops, one which is trivial, i.e., can be continuously deformed to a point, and one which is trivial only when traversed twice. These two types of loops are illustrated in Figure 5 and correspond to the two topological phase factors $+1$ and -1 , respectively, first discovered by Milman and Mosseri⁴⁵.

The second feature demonstrates that f is the GP associated with the loop since the accumulation of local phase changes along the path vanishes. However, the local phase changes vanish only for maximally entangled states; for more general two-qubit states $|\psi\rangle = a|00\rangle + b|01\rangle + c|10\rangle + d|11\rangle$, the global phase factors contain also dynamical contributions, i.e.,

$$i \int_0^\tau \langle \psi | \dot{\psi} \rangle dt = i \int_0^\tau \text{Tr} \left(\rho_A U^\dagger \dot{U} \right) dt + i \int_0^\tau \text{Tr} \left(\rho_B V^\dagger \dot{V} \right) dt \neq 0, \quad (57)$$

since $\rho_A \neq \frac{1}{2} \hat{1}_A$ and $\rho_B \neq \frac{1}{2} \hat{1}_B$ if $|\psi\rangle$ is non-maximally entangled, i.e., if $2|ad - bc| < 1$.

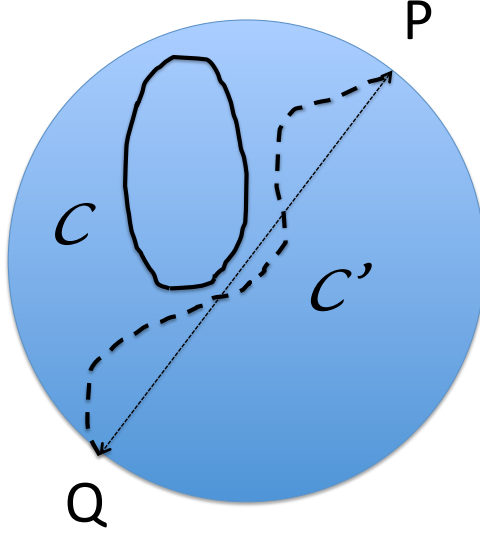


Figure 5: Illustrating the two classes of topologically inequivalent loops in $S^3/Z_2 \simeq \text{SO}(3)$. The loop \mathcal{C} (solid line) can be continuously deformed to a point and correspond to the trivial phase factor $+1$. On the other hand, \mathcal{C}' (dashed line) can be continuously deformed to a point only when traversed twice and correspond to the non-trivial phase factor -1 . Note that \mathcal{C}' is a loop since antipodal points on the sphere are identified, i.e., P and Q are actually the same point.

Note that the allowed cyclic phases f are still 0 or π for any non-vanishing degree of entanglement. The only exception is when $|\psi\rangle$ is a product state, i.e., when $ad - bc = 0$, in case of which a continuum of cyclic phases f may occur under local $\text{SU}(2)$ evolution. Thus, the topological nature of the allowed global phases f is intimately related to entanglement, in the sense that f is no longer a discrete quantity exactly when $|\psi\rangle$ ceases to be entangled. Note that the degree-2 polynomial $ad - bc$ is the determinant of the expansion coefficient, which, as noted above, is known to be a SLOOC and thereby local SU invariant.

The topological two-qubit phases have been generalized by Oxman and Khoury to pairs of d -level systems (qudits)⁴⁶ and pairs of systems with different dimension¹⁶⁰. For equal

dimension, they found the allowed phase factors to be the d th roots of unity

$$e^{if} = e^{iq(2\pi/d)}, \quad q = 0, 1, \dots, d-1, \quad (58)$$

and being related to topological properties of $SU(d)$. The above result for qubit-pairs is recovered as the special case where $d = 2$.

The discrete set of phases in Eq. (58) can be understood as follows. Let the initial state take the general form $|\psi(0)\rangle = \sum_{k,l=1}^d \alpha_{kl} |kl\rangle$. Define the $d \times d$ matrix α with components α_{kl} . A local $SU(d)$ evolution $|\psi(0)\rangle \rightarrow U(t) \otimes V(t) |\psi(0)\rangle$ can be translated into the matrix evolution $\alpha \mapsto \mathbf{u}(t)\alpha\mathbf{v}^T(t)$, where $\mathbf{v}(t)$ and $\mathbf{u}(t)$ are $SU(d)$ matrices with elements $u_{kl}(t) = \langle k|U(t)|l\rangle$ and $v_{kl}(t) = \langle k|V(t)|l\rangle$. Now, a cyclic evolution $|\psi(\tau)\rangle = e^{if}|\psi(0)\rangle$ yields $\mathbf{u}(\tau)\alpha\mathbf{v}^T(\tau) = e^{if}\alpha$. By taking the determinant of this expression, we obtain

$$\det[\mathbf{u}(\tau)] \det[\alpha] \det[\mathbf{v}^T(\tau)] = \det[\alpha] = (e^{if})^d \det[\alpha], \quad (59)$$

where we have used that $\det[\mathbf{u}(\tau)] = \det[\mathbf{v}^T(\tau)] = 1$ for $SU(d)$ matrices. If $\det[\alpha] \neq 0$, we thus obtain that $(e^{if})^d = 1$, which implies Eq. (58). On the other hand, if $\det[\alpha] = 0$, which happens if and only if $|\psi(0)\rangle$ is a product state, then f can take any value and is thereby no longer topological. Note that this is consistent with the result we found in the two-qubit case discussed above.

Topological phases of entangled systems: multi-qubit case

The topological phase structure of multi-qubit systems undergoing local $SU(2)$ evolution has been examined⁴⁷. These phases show a considerably richer structure than those in the bipartite case, due to the richer entanglement structure of systems consisting of more than two particles.

As an illustration of this additional richness, let us consider the simplest case of three qubits in some detail. Here, the allowed topological phases are $0, \frac{\pi}{2}, \pi, \frac{3\pi}{2}$. To understand the reason why just these phases, let us consider an arbitrary three-qubit pure state

$\sum_{klm} \alpha_{klm} |klm\rangle$. The hyperdeterminant of the expansion coefficients α_{klm} takes the form

$$\begin{aligned} \text{Det}[\alpha_{klm}] &= \alpha_{000}^2 \alpha_{111}^2 + \alpha_{001}^2 \alpha_{110}^2 + \alpha_{010}^2 \alpha_{101}^2 + \alpha_{100}^2 \alpha_{011}^2 \\ &\quad - 2(\alpha_{000} \alpha_{001} \alpha_{110} \alpha_{111} + \alpha_{000} \alpha_{010} \alpha_{101} \alpha_{111} + \alpha_{000} \alpha_{100} \alpha_{011} \alpha_{111} \\ &\quad + \alpha_{001} \alpha_{010} \alpha_{101} \alpha_{110} + \alpha_{001} \alpha_{100} \alpha_{011} \alpha_{110} + \alpha_{010} \alpha_{100} \alpha_{011} \alpha_{101}) \\ &\quad + 4(\alpha_{000} \alpha_{011} \alpha_{101} \alpha_{110} + \alpha_{001} \alpha_{010} \alpha_{100} \alpha_{111}), \end{aligned} \quad (60)$$

which apparently is a degree-4 polynomial. Just as $\det[\alpha_{kl}]$ in the bipartite case, $\text{Det}[\alpha_{klm}]$ is a SLOCC invariant; in fact, it determines the 3-tangle $\tau_3 = 4 |\text{Det}[\alpha_{klm}]|$. The 3-tangle measures the amount of genuine three-qubit entanglement in the state¹⁵⁰.

Now, given a cyclic local unitary evolution where all $\alpha_{klm} \rightarrow e^{if} \alpha_{klm}$, we obtain $\text{Det}[\alpha_{klm}] \rightarrow \text{Det}[\alpha_{klm}] = (e^{if})^4 \text{Det}[\alpha_{klm}]$ by using the local SU invariance of $\text{Det}[\alpha_{klm}]$. Thus, provided $\text{Det}[\alpha_{klm}] \neq 0$, we find $(e^{if})^4 = 1$, which implies

$$f = q(2\pi/4), \quad q = 0, \dots, 3. \quad (61)$$

As in the bipartite case, we see that f can take any value and whereby losing its topological nature, in cases where $\text{Det}[\alpha_{klm}] = 0$, which is exactly when three-qubit entanglement is lost (i.e., $\tau_3 = 0$). In this sense, the topological phase f is a genuine property of three-qubit entanglement.

By looking at the space of all pure inseparable three-qubit states, we note that the W -states is a zero measure set of this space with vanishing 3-tangle. The W -set constitutes a singularity in the space of entangled three qubits, just as the singularity line defined by the magnetic solenoid that gives rise to the Aharonov-Bohm topological phase¹⁷⁹. This further illustrates the topological nature of the allowed f for non-vanishing 3-tangle.

The number of allowed topological phases increases with the number of qubits. They have been found for up to seven qubits by using a search algorithm based on a combinatorial formulation of the problem⁴⁷. For eight or more qubits, only partial results have been established due to rapid increase in the computational resources needed to execute the algorithm when the number of qubits increases.

Finally, we note that the multi-qubit phases may coincide with the corresponding GPs. As in the bipartite case, this happens precisely when all the marginal one-qubit states are random mixtures.

Experiments on topological phases of entangled systems

Souza *et al.*¹⁸⁰ (see also¹⁸¹) have used an optical setup involving non-separable polarization and orbital degrees of freedom to simulate quantum entanglement in a laser beam. The laser beam states relevant for this experiment can be described by multiplying orthogonal polarization unit vectors ϵ_H and ϵ_V (horizontal and vertical polarization, respectively) with a pair of first order Laguerre-Gaussian profiles $\psi_{\pm}(\mathbf{r})$ to define the laser beam amplitude

$$\mathbf{E}(\mathbf{r}) = \frac{1}{\sqrt{2}} \left(\alpha \psi_+(\mathbf{r}) \epsilon_H + \beta \psi_+(\mathbf{r}) \epsilon_V - \beta^* \psi_-(\mathbf{r}) \epsilon_H + \alpha^* \psi_-(\mathbf{r}) \epsilon_V \right) \quad (62)$$

representing an arbitrary maximally non-separable (MNS) mode, being a laser beam analog of MES for two-qubit systems. Here, α, β are complex numbers such that $|\alpha|^2 + |\beta|^2 = 1$. All these states are locally equivalent in the sense that any MNS mode can be reached by manipulating only the polarization, say, of the beam. This fact was utilized in¹⁸⁰ to implement loops in the space of MNS modes by letting the laser beam pass a sequence of wave plates. In this way, the topological phases associated with these polarization transformations were realized and observed.

An analogous experiment to observe the topological two-qubit phase for MES has been performed by using NMR technique¹⁸². The setup consists of two nuclear spin-qubits prepared in a MES and a third ancillary qubit playing the role of the two arms of a Mach-Zehnder type interferometer. The input state $\frac{1}{\sqrt{2}}(|0\rangle + |1\rangle) \otimes |\text{MES}\rangle$ is acted on by a conditional operation that takes only the MES copy connected to the $|1\rangle$ state around a loop. Thus, the three qubit state undergoes the transformation

$$\frac{1}{\sqrt{2}}(|0\rangle + |1\rangle) \otimes |\text{MES}\rangle \rightarrow \frac{1}{\sqrt{2}}(|0\rangle \pm |1\rangle) \otimes |\text{MES}\rangle, \quad (63)$$

where the relative sign is precisely the topological phase factor ± 1 associated with the loop. In this way, the topological phases were read out by measuring the ancilla qubit state¹⁸².

The qudit and multi-qubit phases have not been verified experimentally yet. However, feasible experimental proposals using polarization and orbital degrees of freedom of photon pairs have been put forward^{183,184} and awaits to be performed in the future.

CONCLUSIONS

We have reviewed the role of geometric phase (GP) ideas in quantum information science. We have described how GPs can be used to perform robust quantum information processing, leading to the idea of holonomic or geometric quantum computation, which is a tool to realize quantum gates that are robust to certain errors. GP concepts for mixed quantum states have been described, focusing on Uhlmann's seminal work from the mid 1980s and the more recent development of mixed state GPs in interferometry. Finally, we have described how GPs can be used to analyze quantum entanglement, with particular focus on the discovery of a new type of topological phases for entangled systems.

The importance of the reviewed body of work is two-fold. It has led to new ways to perform quantum information processing that may be useful to fight errors in quantum gate operations. This may help to reach below the error threshold, below which quantum error correction codes can be performed. In other words, GPs may help to realize large-scale quantum computation. Conversely, ideas that have been developed or refined within the quantum information community, such as the theory of mixed quantum states, open system effects, and quantum entanglement, have been applied to the theory of GP. In this way, further insights into the physical, mathematical, and conceptual nature of the GP have been obtained.

There are a number of pertinent issues to examine in the future in this research area. First, explicit physical implementations of schemes that combine GQC and symmetry-aided error protection techniques such as decoherence free subspaces and subsystems, need to be developed and experimentally implemented. The key question here is whether there exist such schemes that at the same time avoid many-body interaction terms in the Hamiltonian and thereby would be much simpler to realize in the laboratory than the existing schemes. Secondly, the conjectured robustness of GQC compared to more conventional dynamical quantum gates is still an open problem that needs to be examined further. In particular, the robustness features of geometric gates in the presence of open system effects need to be addressed in realistic models that include significant non-Markovian effects. Thirdly, the relation between the interferometric-based and Uhlmann GPs is still not fully understood. A

key goal here is to find a common conceptual basis for these two phases, such as for instance a new mixed state GP concept that covers the two. Finally, a major challenge concerning GP effects in entangled systems is to clarify the relation between the entanglement-induced topological phases and SLOCC invariant polynomials of multi-qubit systems and to implement experimentally these phases in the qudit and multi-qubit cases. Addressing the above listed open problems would lead to further insights into the nature of the GP and to new applications of GP ideas in quantum information science.

ACKNOWLEDGMENTS

I wish to thank Jeeva Anandan, Mauritz Andersson, Vahid Azimi Mousolou, Johan Brännlund, Carlo Canali, Artur Ekert, Marie Ericsson, Björn Hessmo, Markus Johansson, Antonio Khoury, David Kult, Leong Chuan Kwek, Peter Larsson, Daniel Oi, Oh Choo Hiap, Arun Pati, Patrik Pawlus, Kuldip Singh, Jakob Spiegelberg, Anthony Sudbery, Patrik Thunström, Dianmin Tong, Vlatko Vedral, Mark Williamson, William Wootters, Paolo Zanardi, Guofu Xu, Jiang Zhang, and Johan Åberg for fruitful collaboration over the years on geometric phase issues related to this review. Financial support from the Swedish Research Council (Vetenskapsrådet) is acknowledged.

References

1. Shapere, A., Wilczek, F., Am. J. Phys. **1989**, 57, 514-518.
2. Shapere, A., Wilczek, F., J. Fluid Mech. **1989**, 198, 557-585.
3. Batterman, R. W., Stud. Hist. Phil. Science B **2003**, 34, 527-557.
4. Longuet-Higgins, H. C., Öpik, U., Pryce, M. H. L., Sack, R. A., Proc. R. Soc. London, Ser. A **1958**, 244, 1-16.
5. Herzberg, G., Longuet-Higgins, H. C., Faraday Soc. Discuss. **1963**, 35, 77-82.
6. Longuet-Higgins, H. C., Proc. R. Soc. London, Ser. A **1975**, 344, 147-156.
7. Stone, A. J., Proc. R. Soc. London, Ser. A **1976**, 351, 141-150.
8. Mead, C. A., Chem. Phys. **1980**, 49, 23-32.
9. Mead, C. A., Chem. Phys. **1980**, 49, 33-38.
10. Berry, M. V., Proc. R. Soc. London Ser. A **1984**, 392, 45-57.
11. Tomita, A., Chiao, R. Y., Phys. Rev. Lett. **1986**, 57, 937-940.
12. Suter, D., Chingas, G., Harris, R. A., Pines, A., Mol. Phys. **1987**, 61, 1327-1340.
13. Bitter, T., Dubbers, D., Phys. Rev. Lett. **1987**, 59, 251-254.
14. von Busch, H., Dev, V., Eckel, H.-A., Kasahara, S., Wang, J., Demtröder, W., Sebald, P., Meyer, W., Phys. Rev. Lett. **1998**, 81, 4584-4587.
15. Zhang, Y., Tan, Y.-W., Stormer, H. L., Kim, P. Nature **2005**, 438, 201-204.
16. Lin, Y.-J., Compton, R. L., Jiménez- García, K., Porto, J. V., Spielman, I. B., Nature **2009**, 462, 628-632.
17. Simon, B., Phys. Rev. Lett. **1984**, 51, 2167-2170.
18. Wilczek, F., Zee, A., Phys. Rev. Lett. **1984**, 52, 2111-2114.

19. Aharonov, Y., Anandan, J., Phys. Rev. Lett. **1987**, 58, 1593-1596.
20. Anandan, J., Phys. Lett. A **1988**, 133, 171-175.
21. Pancharatnam, S., Proc. Ind. Acad. Sci. A **1956**, 44, 247-262.
22. Samuel, J., Bhandari, R., Phys. Rev. Lett. **1988**, 60, 2339-2342.
23. Vedral, V., Int. J. Quantum Inf. **2003**, 1, 1-24.
24. Sjöqvist, E., Physics **2008**, 1, 35.
25. Zanardi, P., Rasetti, M., Phys. Lett. A **1999**, 264, 94-99.
26. Pachos, J., Zanardi, P., Rasetti, M., Phys. Rev. A **1999**, 61, 010305(R).
27. Pachos, J., Zanardi, P., Int. J. Mod. Phys. B **2001**, 15, 1257-1285
28. Uhlmann, A., Rep. Math. Phys. **1986**, 24, 229-240.
29. Sjöqvist, E., Pati, A. K., Ekert, A., Anandan, J. S., Ericsson, M., Oi, D. K. L., Vedral, V., Phys. Rev. Lett. **2000**, 85, 2845-2849.
30. Tong, D. M., Sjöqvist, E., Kwek, L. C., Oh, C. H., Phys. Rev. Lett. **2004**, 93, 080405.
31. Marzlin, K.-P., Ghose, S., Sanders, B. C., Phys. Rev. Lett. **2004**, 93, 260402.
32. Chaturvedi, S., Ercolessi, E., Marmo, G., Morandi, G., Mukunda, N., Simon, R., European Phys. J. C **2004**, 35, 413-423.
33. Carollo, A., Fuentes-Guridi, I., Santos, M. F., Vedral, V., Phys. Rev. Lett. **2003**, 90, 160402.
34. Fuentes-Guridi, I., Girelli, F., Livine, E., Phys. Rev. Lett. **2005**, 94, 020503.
35. Peixoto de Faria, J. G., de Toledo Piza, A. F. R., Nemes, M. C., EPL **2003**, 62, 782-788.
36. Ericsson, M., Sjöqvist, E., Brännlund, J., Oi, D. K. L., Pati, A. K., Phys. Rev. A **2003**, 67, 020101.

37. Kult, D., Åberg, J., Sjöqvist, E., Phys. Rev. A **2008**, 77, 012114.
38. Bassi, A., Ippoliti, E., Phys. Rev. A **2006**, 73, 062104.
39. Sjöqvist, E., Acta Phys. Hung. B **2006**, 26, 195-201.
40. Burić, N., Radonjić, M., Phys. Rev. A **2009**, 80, 014101.
41. Pawlus, P., Sjöqvist, E., Phys. Rev. A **2010**, 82, 052107.
42. Thunström, P., Åberg, J., Sjöqvist, E., Phys. Rev. A **2005**, 72, 022328.
43. Sarandy, M. S., Lidar, D. A., Phys. Rev. A **2006**, 73, 062101.
44. Oreshkov, O., Calsamiglia, J., Phys. Rev. Lett. **2010**, 105, 050503.
45. Milman, P., Mosseri, R., Phys. Rev. Lett. **2003**, 90, 230403.
46. Oxman, L. E., Khoury, A. Z., Phys. Rev. Lett. **2011**, 106, 240503.
47. Johansson, M., Ericsson, M., Singh, K., Sjöqvist, E., Williamson, M. S., Phys. Rev. A **2012**, 85, 032112.
48. Mukunda, N., Simon, R., Ann. Phys. (N.Y.) **1993**, 228, 205-268.
49. Wagh, A. G., Rakhecha, V. C., Phys. Lett. A **1995**, 197, 107-111.
50. Wagh, A. G., Rakhecha, V. C., Phys. Lett. A **1995**, 197, 112-115.
51. Wagh, A. G., Rakhecha, V. C., Fischer, P., Ioffe, A., Phys. Rev. Lett. **1998**, 81, 1992-1995.
52. Pati, A. K., J. Phys. A **1995**, 28, 2087-2094.
53. Pati, A. K., Phys. Rev. A **1995**, 52, 2576-2584.
54. Kult, D., Åberg, J., Sjöqvist, E., Phys. Rev. A **2006**, 74, 022106.
55. Unanyan, R. G., Shore, B. W., Bergmann, K., Phys. Rev. A **1999**, 59, 2910-2919.
56. Knill, E., Nature (London) **2005**, 434, 39-44.

57. Shor, P. W., Phys. Rev. A **1995**, 52, R2493-R2496.
58. Steane, A. M., Phys. Rev. Lett. **1996**, 77, 793-797.
59. Bremner, M. J., Dawson, C. M., Dodd, J. L., Gilchrist, A., Harrow, A. W., Mortimer, D., Nielsen, M. A., Osborne, T. J., Phys. Rev. Lett. **2002**, 89, 247902.
60. Zhu, S.-L., Wang, Z. D., Phys. Rev. Lett. **2002**, 89, 097902.
61. Zhu, S.-L., Wang, Z. D., Phys. Rev. A **2003**, 67, 022319.
62. Sjöqvist, E., Tong, D. M., Andersson, L. M., Hessmo, B., Johansson, M., Singh, K., New J. Phys. **2012**, 14, 103035.
63. Jones, J. A., Vedral, V., Ekert, A., Castagnoli, G., Nature (London) **1999**, 403, 869-871.
64. Ekert, A., Ericsson, M., Hayden, P., Inamori, H., Jones, J. A., Oi, D. K. L., Vedral, V., J. Mod. Opt. **2000**, 47, 2501-2513.
65. Zhu, S.-L., Zanardi, P., Phys. Rev. A **2005**, 72, 020301(R).
66. Tian, M., Barber, Z. W., Fischer, J. A., Babbitt, W. R., Phys. Rev. A **2004**, 69, 050301(R).
67. Zhu, S.-L., Wang, Z. D., Phys. Rev. Lett. **2003**, 91, 187902.
68. Leibfried, D., DeMarco, B., Meyer, V., Lucas, D., Barrett, M., Britton, J., Itano, W. M., Jelenković, B., Langer, C., Rosenband, T., Wineland, D. J., Nature (London) **2002**, 422, 412-415.
69. Du, J., Zou, P., Wang, Z. D., Phys. Rev. A **2006**, 74, 020302(R).
70. Duan, L.-M., Cirac, J. I., Zoller, P., Science **2001**, 292, 1695-1697.
71. Recati, A., Calarco, T., Zanardi, P., Cirac, J. I., Zoller, P., Phys. Rev. A **2002**, 66, 032309.
72. Faoro, L., Siewert, J., Fazio, R., Phys. Rev. Lett. **2003**, 90, 028301.

73. Solinas, P., Zanardi, P., Zanghì, N., Rossi, F., Phys. Rev. B **2003**, 67, 121307.
74. Azimi Mousolou, V., Canali, C. M., Sjöqvist, E., New J. Phys. **2014**, 16, 013029.
75. Güngördü, U., Wan, Y., Nakahara, M., J. Phys. Soc. Jpn. **2014**, 83, 034001.
76. Malinovsky, V., Rudin, S., Phys. Scr. **2014**, T160, 014029.
77. Pachos, J., Walther, H., Phys. Rev. Lett. **2002**, 89, 187903.
78. Møller, D., Madsen, L. B., Mølmer, K., Phys. Rev. A **2007**, 75, 062302.
79. Niskanen, A. O., Nakahara, M., Salomaa, M. M., Phys. Rev. A **2003**, 67, 012319.
80. Karle, R., Pachos, J., J. Math. Phys. **2003**, 44, 2463-2470.
81. Tanimura, S., Hayashi, D., Nakahara, M., Phys. Lett. A **2004**, 325, 199-205.
82. Pirkkalainen, J.-M., Solinas, P., Pekola, J. P., Möttönen, M., Phys. Rev. B **2010**, 81, 174506.
83. Sørensen, A., Mølmer, K., Phys. Rev. Lett. **1999**, 82, 1971-1974.
84. Abdumalikov Jr., A. A., Fink, J. M., Juliusson, K., Pechal, M., Berger, S., Wallraff, A., Filipp, S., Nature (London) **2013**, 496, 482-485.
85. Feng, G., Xu, G., Long, G., Phys. Rev. Lett. **2013**, 110, 190501.
86. Arroyo-Camejo, S., Lazareiev, A., Hell, S. W., Balasubramanian, G., Nature Comm. **2014**, 5, 4870.
87. Zu, C., Wang, W.-B., He, L., Zhang, W.-G., Dai, C.-Y., Wang, F., Duan, L.-M., Nature (London) **2014**, 512, 72-75.
88. Xu, G. F., Zhang, J., Tong, D. M., Sjöqvist, E., Kwek, L. C., Phys. Rev. Lett. **2012**, 109, 170501.
89. Wootters, W. K., Phys. Rev. Lett. **1998**, 80, 2245-2248.

90. Toyoda, K., Uchida, K., Noguchi, A., Haze, S., Urabe, S., Phys. Rev. A **2013**, 87, 052307.
91. Nazir, A., Spiller, T. P., Munro, W. J., Phys. Rev. A **2002**, 65, 042303.
92. Blais, A., Tremblay, A.-M. S., Phys. Rev. A **2003**, 67, 012308.
93. Trullo, A., Facchi, P., Fazio, R., Florio, G., Giovanetti, V., Pascazio, S., Laser Phys. **2006**, 16, 1478-1485.
94. Florio, G., Facchi, P., Fazio, R., Giovannetti, V., Pascazio, S., Phys. Rev. A **2006**, 73, 022327.
95. Lupo, C., Aniello, P., Napolitano, M., Florio, G., Phys. Rev. A **2007**, 76, 012309.
96. Johansson, M., Sjöqvist, E., Andersson, L. M., Ericsson, M., Hessmo, B., Singh, K., Tong, D. M., Phys. Rev. A **2012**, 86, 062322.
97. Spiegelberg, J., Sjöqvist, E., Phys. Rev. A **2013**, 88, 054301.
98. De Chiara, G., Massimo Palma, G., Phys. Rev. Lett. **2003**, 91, 090404.
99. Leek, P. J., Fink, J. M., Blais, A., Bianchetti, R., Göppl, M., Gambetta, J. M., Schuster, D. I., Frunzio, L., Schoelkopf, R. J., Wallraff, A., Science **2007**, 318, 1889-1892.
100. Berger, S., Pechal, M., Abdumalikov Jr., A. A., Eichler, C., Steffen, L., Fedorov, A., Wallraff, A., Filipp, S., Phys. Rev. A **2013**, 87, 060303(R).
101. Filipp, S., Klepp, J., Hasegawa, Y., Plonka-Spehr, C., Schmidt, U., Geltenbort, P., Rauch, H., Phys. Rev. Lett. **2009**, 102, 030404.
102. Wu, L.-A., Zanardi, P., Lidar, D. A., Phys. Rev. Lett. **2005**, 95, 130501,
103. Oreshkov, O., Phys. Rev. Lett. **2009**, 103, 090502.
104. Renes, J. M., Miyake, A., Brennen, G. K., Bartlett, S. D., New J. Phys. **2013**, 15, 025020.

105. Zheng, Y.-C., Brun, T. A., Phys. Rev A **2014**, 89, 032317.
106. Zheng, Y.-C., Brun, T. A., Phys. Rev A **2015**, 91, 022302.
107. Zanardi, P., Rasetti, M., Phys. Rev. Lett. **1997**, 79, 3306-3309.
108. Lidar, D. A., Chuang, I. L., Whaley, K. B., Phys. Rev. Lett. **1998**, 81, 2594-2597.
109. Knill, E., Laflamme, R., Viola, L., Phys. Rev. Lett. **2000**, 84, 2525-2528.
110. Zhang, J., Kwek, L. C., Sjöqvist, E., Tong, D. M., Zanardi, P., Phys. Rev A **2014**, 89, 042302.
111. Oreshkov, O., Brun, T. A., Lidar, D. A., Phys. Rev. Lett. **2009**, 102, 070502.
112. Oreshkov, O., Brun, T. A., Lidar, D. A., Phys. Rev. A **2009**, 80, 022325.
113. Jordan, S. P., Fahri, E., Phys. Rev. Lett. **2008**, 77, 062329.
114. Xu, G., Long, G., Sci. Rep. **2014**, 4, 6814.
115. Xu, G., Long, G., Phys. Rev. A **2014**, 90, 022323.
116. Viola, L., Knill, E., Lloyd, S., Phys. Rev. Lett. **1999**, 82, 2417-2421.
117. Lindblad, G., Commun. Math. Phys. **1973**, 48, 119-130.
118. Singh, K., Tong, D. M., Basu, K., Chen, J. L., Du, J., Phys. Rev. A **2003**, 67, 032106.
119. Lombardo, F. C., Villar, P. I., Phys. Rev. A **2006**, 74, 042311.
120. Yi, X. X., Wang, L. C., Kwek, L. C., Oh, C. H., Phys. Rev. A **2006**, 74, 052103.
121. Baerjee, S., Srikanth, R., Eur. Phys. J. D **2008**, 46, 335-344.
122. Dajka, J., Łuczka, J., Hänggi, P., Quantum Inf. Process. **2011**, 10, 85-96.
123. Uhlmann, A., Lett. Math. Phys. **1991**, 21, 229-236.
124. Hübner, M., Phys. Lett. A **1993**, 179, 226-230.

125. Uhlmann, A., Rep. Math. Phys. **1976**, 9, 273-279.
126. Ericsson, M., Pati, A. K., Sjöqvist, E., Brännlund, J., Oi, D. K. L., Phys. Rev. Lett. **2003**, 91, 090405.
127. Åberg, J., Kult, D., Sjöqvist, E., Oi, D. K. L., Phys. Rev. A **2007**, 75, 032106.
128. Viyuela, O., Rivas, A., Martin-Delgado, M. A., Phys. Rev. Lett. **2014**, 112, 130401.
129. Huang, Z., Arovas, D. P., Phys. Rev. Lett. **2014**, 113, 076407.
130. Viyuela, O., Rivas, A., Martin-Delgado, M. A., Phys. Rev. Lett. **2014**, 113, 076408.
131. Slater, P. B., Lett. Math. Phys. **2002**, 60, 123-133.
132. Shi, M., Du, J., **2005**, arxiv:quant-ph/0501006.
133. Andersson, O., Heydari, H., **2014**, arXiv:1411.0635.
134. Reza khani, A., Zanardi, P., Phys. Rev. A **2006**, 73, 012107.
135. Bhandari, R., Phys. Rev. Lett. **2002**, 89, 268901.
136. Anandan, J., Sjöqvist, E., Pati, A. K., Ekert, A., Ericsson, M., Oi, D. K. L., Vedral, V., Phys. Rev. Lett. **2002**, 89, 268902.
137. Du, J., Zou, P., Shi, M., Kwek, L. C., Pan, J.-W., Oh, C. H., Ekert, A., Oi, D. K. L., Ericsson, M., Phys. Rev. Lett. **2003**, 91, 100403.
138. Ghosh, A., Kumar, A., Phys. Lett. A **2006**, 349, 27-36.
139. Cucchietti, F. M., Zhang, J.-F., Lombardo, F. C., Villar, P. I., Laflamme, R. Phys. Rev. Lett. **2010**, 105, 240406.
140. Ericsson, M., Achilles, D., Barreiro, J. T., Branning, D., Peters, N. A., Kwiat, P. G., Phys. Rev. Lett. **2005**, 95, 050401.
141. dEspagnat, B., Conceptual Foundations of Quantum Mechanics; Addison Wesley **1976**.

142. Larsson, P., Sjöqvist, E., Phys. Lett. A **2003**, 315, 12-15.
143. Klepp, J., Sponar, S., Hasegawa, Y., Jericha, E., Badurek, G., Phys. Lett. A **2005**, 342, 48-52.
144. Klepp, J., Sponar, S., Filipp, S., Lettner, M., Badurek, G., Hasegawa, Y., Phys. Rev. Lett. **2008**, 101, 150404.
145. Zhu, J., Shi, M., Vedral, V., Peng, X., Suter, D., Du, J., EPL **2011**, 94, 20007.
146. Ekert, A., Phys. Rev. Lett. **1991**, 67, 661-663.
147. Bennett, C. H., Brassard, G., Crépeau, C., Jozsa, R., Peres, A., Wootters, W. K., Phys. Rev. Lett. **1993**, 70, 1895-1899.
148. Raussendorf, R., Briegel, H. J., Phys. Rev. Lett. **2001**, 86, 5188-5191.
149. Dür, W., Vidal, G., Cirac, J. I., Phys. Rev. A **2000**, 62, 062314.
150. Coffman, V., Kundu, J., Wootters, W. K., Phys. Rev. A **2000**, 61, 052306.
151. Bennett, C. H., DiVincenzo, D. P., Smolin, J. A., Wootters, W. K., Phys. Rev. A **1996**, 54, 3824-3851.
152. Shimony, A., Ann. N.Y. Acad. Sci. **1995**, 755, 675.
153. Wei, T.-C., Goldbart, P. M., Phys. Rev. A **2003**, 68, 042307.
154. Vedral, V., Plenio, M. B., Rippin, M. A., Knight, P. L., Phys. Rev. Lett. **1997**, 78, 2275-2279.
155. Luque, J.-G., Thibon, J.-Y., Phys. Rev. A **2003**, 67, 042303.
156. Đoković, D. Ž., Osterloh, A., J. Math. Phys. **2009**, 50, 033509.
157. De Zela, F., J. Opt. B: Quantum Semiclass. Opt. **2005**, 7, 372-380.
158. LiMing, W., Tang, Z. L., Liao, C. J., Phys. Rev. A **2004**, 69, 064301.

159. Milman, P., Phys. Rev. A **2006**, 73, 062118.
160. Khoury, A. Z., Oxman, L. E., Phys. Rev. A **2014**, 89, 032106.
161. Oxman, L. E., Khoury, A. Z., Ann.Phys. (N. Y.) **2014**, 351, 138-151.
162. Sjöqvist, E., Phys. Rev. A **2000**, 62, 022109.
163. Tong, D. M., Kwek, L. C., Oh, C. H., J. Phys. A: Math. Gen. **2003**, 36, 1149-1157.
164. Chen, J.-L., Xue, K., Ge, M.-L., Phys. Rev. A **2007**, 76, 042324.
165. Loredó, J. C., Broome, M. A., Smith, D. H., White, A. G., Phys. Rev. Lett. **2014**, 112, 143603.
166. Tong, D. M., Sjöqvist, E., Kwek, L. C., Oh, C. H., Ericsson, M., Phys. Rev. A **2003**, 68, 022106.
167. Williamson, M. S., Vedral, V., Phys. Rev. A **2007**, 76, 032115.
168. Wootters, W. K., J. Math. Phys. **2002**, 43, 4307.
169. Williamson, M. S., Ericsson, M., Johansson, M., Sjöqvist, E., Sudbery, A., Vedral, V., Wootters, W. K., Phys. Rev. A **2011**, 83, 062308.
170. Williamson, M. S., Ericsson, M., Johansson, M., Sjöqvist, E., Sudbery, A., Vedral, V., Phys. Rev. A **2011**, 84, 032302.
171. Sjöqvist, E., EPL **2009**, 86, 30005.
172. Sjöqvist, E., Phys. Lett. A **2010**, 374, 1431-1433.
173. Bertlmann, R. A., Durstberger, K., Hasegawa, Y., Hiesmayr, B. C., Phys. Rev. A **2004**, 69, 032112.
174. Sponar, S., Klepp, J., Loidl, R., Philipp, S., Durstberger-Rennhofer, K., Bertlmann, R. A., Badurek, G., Rauch, H., Hasegawa, Y., Phys. Rev. A **2010**, 81, 042113.
175. Basu, B., EPL **2006**, 73, 833-838.

176. Mosseri, R., Dandaloff, R., J. Phys. A: Math. Gen. **2001**, 34, 10243-10252.
177. Lévy, P., J. Phys. A: Math. Gen. **2004**, 37, 1821-1842.
178. Johansson, M., Ericsson, M., Singh, K., Sjöqvist, E., Williamson, M. S., J. Phys. A: Math. Theor. **2011**, 44, 145301.
179. Aharonov, Y., Bohm, D., Phys. Rev. **1959**, 115, 485-491.
180. Souza, C. E. R., Huguenin, J. A. O., Milman, P., Khoury, A. Z., Phys. Rev. Lett. **2007**, 99, 160401.
181. Souza, C. E. R., Huguenin, J. A. O., Khoury, A. Z., J. Opt. Soc. Am. A **2014**, 31, 1007-1012.
182. Du, J., Zhu, J., Shi, M, Peng, X, Suter, D., Phys Rev. A **2007**, 76, 042121.
183. Johansson, M., Khoury, A. Z., Singh, K., Sjöqvist, E., Phys. Rev. A **2013**, 87, 042112.
184. Khoury, A. Z., Oxman, L. E., Marques, B., Matoso, A., Pádua, S., Phys. Rev. A **2013**, 87, 042113.